Summer Programs Symposium

August 2nd – August 3rd, 2023

Abstract Booklet

Summer Program for Undergraduate Research (SPUR)

John Obiefuna – University of North Carolina at Chapel Hill

Aprill Z Dawson, Ph.D, MPH; Abigail Thorgerson; Sebastian Linde; Rebekah J. Walker, Ph.D; Sanjay Bhandari, MD; Leonard Egede, MD, MS

MCW Center of Advancing Population Science

Healthcare utilization in older adults with diabetes and dementia: Medical Expenditure Panel Survey (2000 – 2020)

Background and Significance

Adults with diabetes have two times the risk of developing dementia compared to adults without diabetes. The aim of this analysis was to determine the rates of healthcare utilization in older adults with diabetes and dementia.

Methods

Data representing 102,176,914 adults aged 50 and older from the Medical Expenditure Panel Survey (2000-2020) were used. Inpatient, outpatient, emergency, dental, pharmacy, home-health, and total medical visits were dependent variables. The primary independent variable had 4 categories: no diabetes or dementia, diabetes only, dementia only, comorbid diabetes and dementia (DD). Covariates included age, race/ethnicity, sex, marital status, education, region, poverty, comorbidities, and survey year. Unadjusted and fully adjusted two-part models with gamma family and log link models were run. Analyses were conducted using Stata v17.0, and statistical significance was p-value<0.05.

Results

In fully adjusted models, those with diabetes only (mean:$6284;95%CI:$6053,$6515), dementia only (mean:$8226;95%CI:$7151,$9302), and DD (mean:$8487.31;95%CI:$6558,$10417) had significantly higher total expenditures compared to individuals without diabetes or dementia. In addition, those with diabetes only (mean:$2286;95%CI:$2160,$2413), dementia only (mean:$2316;95%CI:$2003,$2629), and DD (mean:$2998;95%CI:$2304,$3692) had significantly higher prescription expenditures compared to individuals without diabetes or dementia. Older adults with dementia only had higher ED expenditures (mean:$395;95%CI:$261,$529). Older adults with dementia only (mean: $758;95%CI:$562,$953) and co-morbid diabetes and dementia (mean: $633;95%CI:$370,$896) had higher home health expenditures compared to individuals with neither condition.

Summary and Conclusion

Adults aged 50 and older with comorbid diabetes and dementia have significantly higher rates of inpatient, pharmacy, and home health utilization compared to older adults with neither condition. In addition, having dementia is a key driver of healthcare utilization among adults aged 50 and older in the US.

Liliana De Leon – Alverno College
Helen Files – Medical College of Wisconsin
Cameron Anderson – Medical College of Wisconsin
Michelle Riehle, PhD
MCW Department of Microbiology and Immunology

Regulating Resistance: Examining Candidate Regulatory Elements of the Malaria Resistance Gene, LRIM1

Background

Malaria is a vector-borne disease that causes high morbidity and mortality rates in Africa, especially among children under the age of five. In the vector *Anopheles*, many immune regulated proteins have been discovered. One of these, the leucine-rich repeat immune molecule 1 (LRIM1) protein, works in a three protein complex to decrease the number of *Plasmodium* parasites. This 3 member complex requires the LRIM1 protein for successful opsonization of *Plasmodium*. Currently, little is known about how LRIM1 gene expression is regulated. Using previously generated genome-wide catalogs of enhancers, the goal of this study is to experimentally validate the activity of two candidate enhancers near the LRIM1 gene, measure differences in enhancer activity among resistant and susceptible mosquitoes, and determine how variation in an enhancer sequence can impact differences in activity.

Methods

The luciferase reporter assay was used to measure enhancer activity levels in resistant and susceptible *Anopheles* mosquitoes. The genomic DNA samples were used to PCR amplify and clone enhancer fragments into the reporter vector, pGL3-Gateway-DSCP. Using lipid-based transfection, enhancer containing plasmids were transfected into Ag55 hemocyte-like cells. Twenty-four hours after transfection, luciferase activity was measured, which is a measurement of enhancer activity. Activity levels were statistically compared using analysis of variance (ANOVA) and multiple comparison tests.

Results

Both candidate enhancers showed activity above background in a luciferase assay, which validated results from previous genome wide screens. Enhancer 1 cloned from malaria susceptible mosquitoes was significantly ($p<0.0001$) more active than the clone from malaria resistant mosquitoes. Enhancer 2 cloned from malaria susceptible mosquitoes also showed significantly ($p=0.0222$) higher activity in clones derived from malaria susceptible mosquitoes. Site directed mutagenesis was used to determine the impact of genetic variation within a predicted transcription factor binding site (TFBS) in enhancer 1. Mutation of the predicted TFBS within enhancer 1 resulted in significantly higher activity for the malaria susceptible clone and significantly lower activity for the malaria resistant clone consistent with transcription factor binding at this TFBS negatively affecting overall enhancer activity.

Conclusion

This work focused on two candidate regulatory elements with potential roles in the regulation of LRIM1. Due to its higher activity, enhancer 1 is the stronger candidate for future work determining the role of this enhancer in the natural regulation of a crucial malaria immune gene. Additional studies connecting these results to LRIM1 are on-going and will be vital in the creation of malaria control tools.

Mason Thao – University of Wisconsin Madison
Joel B. Miesfeld, Ph.D.
MCW Department of Ophthalmology and Visual Science

Atoh7 regulation of Pax6 expression during Retinal Ganglion Cell Genesis

Background

The Paired Box 6 (Pax6) gene has been widely studied for its critical involvement in regulating all aspects of early retinal development. Although the gene regulation effects of Pax6 have been well documented, regulation of the expression of Pax6 itself and its role in RGC remains unknown. With a vested interest in understanding the expression of a key transcription factor such as Pax6 in Retinal Ganglion Cell specification, our study aims to analyze shared overlapping genomic regions of 3 transcription factors: Atonal bHLH transcription factor 7 (Atoh7) alongside downstream transcription factors Pou4f2 and Isl-1. We hypothesize that all three transcription factors coordinately regulate the expression of Pax6 due to shared overlapping genomic protein binding regions and that Pax6 is essential for RGC genesis and survival.

Method

Using Lakritz Atoh7 mutant zebrafish models, we aim to demonstrate the function of Pax6 during RGC genesis and survival. A Gibson Assembly was performed to generate a DNA plasmid capable of expressing Pax6 in the Atoh7 lineage using chemically competent bacteria. Subsequently, we performed a DNA extraction of the Pax6-positive bacteria cells for our injection mix. Lakritz Atoh7 +/- mutant zebrafish crosses were then prepared for Pax6 microinjection. Zebrafish embryos were injected with a CNE2-3: Pax6-P2AmCherryPEST mix during the one-cell to four-cell stage. At 48 hpf, all surviving embryos were fixed in a 250 µL 4% PFA/ 1x PBS solution overnight. Collection of embryo heads and tails was performed for immunostaining and genotyping of embryos, respectively. After identifying Lakritz mutants, heterozygous mutants, and wild type embryos, each head was identified and separated into their respective genotypes for immunofluorescence staining of Pax6, mCherry, and the RGC marker Rbpms2. Lastly, confocal microscopy was performed on each embryo's retina, screening for Pax6 expression and RGC via Z-stack imaging.

Results

Z-Stack Confocal microscopy imaging reveals a significantly lower expression of Rbpms2-labeled RGCs and an overall lower activity of mCherry/GFP Pax6 expression found in Lakritz Mutant embryos. Heterozygous and Wild Type control group confocal microscopy imaging revealed a significantly higher and consistent expression of Rbpms2-labeled RGC throughout the retinal ganglion cell layer as well as higher levels of mCherry/GFP Pax6 expression.

Conclusion

Our study suggests that Pax6 does not have a significant regulatory effect on the genesis and survival of RGCs in Lakritz mutant zebrafish retinas. Further investigation into Pou4f2 & Isl-1 is required to understand the obscured and complex nature of the expression and function of the keystone transcription factor Pax6, as well as other target genes, in RGC genesis. Given our

findings, our understanding of Pax6 in RGC expression is yet limited. Further emphasizing the need to better understand the regulatory network of an organ as essential as the eye.

David Ramirez – California State University, Chico
Robert Lochhead, PhD
MCW Department of Microbiology & Immunology

Bacterial peptidoglycan stimulates synovial inflammation in knee osteoarthritis

Background

Knee osteoarthritis (OA) is a disease that approximately affects ⅓ of the population in the US aged 60 years & older. Inflammation at the synovium negatively alters the function of the knee joint & decreases lower extremity movement. A compelling gap must be filled to improve our understanding of the pathogenesis in OA. In a study published recently, we revealed that peptidoglycan (PG), a component of the cell wall in most bacteria was discovered in the synovium of the knee joint in 59% of the patients that had knee OA. We confirmed that levels of PG were associated with synovial inflammation & levels of PG were inversely associated with patient age at the time of total knee arthroplasty (TKA) which can potentially be used as a biomarker. In this study, we aim to detect bacterial DNA using collected synovial tissue biopsies obtained from these patients undergoing TKA. We hypothesize that bacterial DNA will be detected in the biopsies collected & would confirm that the detection of PG in patients with OA is due to low levels of active microbial contamination & therefore is the main driver of inflammation & progresses the rate of the disease.

Method

Total DNA was extracted from the 70 total synovial tissue biopsies using a DNeasy Blood & Tissue Kit (Qiagen). A NanoDrop Spectrophotometer was used to assess & ensure that the DNA was successfully extracted. The unit measured ng/μL was used to observe the concentration amount of DNA in each sample. Our desired range for concentrated DNA was ≥30 ng/μL. The wavelength ratio of A260/A280 was used to assess DNA purification in each sample to ensure that no other contaminants or proteins were in the extracted DNA. Our optimal wavelength range of ratio is ~1.8-2.0.

Results

We observed that 60/70 of the were above the desired range of DNA concentration (≥30 ng/μL) & were also within the A260/A280 optimal ratio of ~1.8-2.0 that assessed purity. Subsequently, to ensure the accurate representation of samples, we repeated the 10/70 samples that did not meet the desired range for concentrated DNA and/or the optimal wavelength ratio. After repeating the 10 samples that did not meet the criteria, we observed that 9/10 samples were brought into their optimal desired ranges & ensured that DNA was sufficiently extracted for each of the 70 biopsies.

Conclusion

Our study shows that DNA was optimally extracted from all synovial tissue biopsies & can be used for further amplification, purification, & analysis under qPCR to determine the presence of bacterial DNA. If bacterial DNA is detected, then we can conclude that inflammatory OA is due to microbial contamination. Future studies will determine whether the bacteria is primarily gram-negative or gram-positive & the specific species as well.

Andrea Herrera – Alverno College
Vera Tarakanova, PhD
MCW Department of Microbiology & Immunology

Effects of IRF3 Deficiency in Macrophages on Type 1 IFN Response

Background

Gammaherpesviruses (GHV) are common pathogens associated with cancers like B cell lymphoma and Kaposi's sarcoma. They are known to establish life-long infections, establish latency in several types of B cells and in macrophages. During pathogenic invasion, gammaherpesviruses alter the innate and adaptive immune responses. IRF3 is a ubiquitous transcription factor that controls activation of various interferon (IFN) genes like type 1 IFN. The first cells to be infected begin with epithelial cells, leading to macrophage infection. The expression of IRF3 in macrophages blocks the MHV68 infection to B cells. When IRF3 is expressed, it leads to the production of Type 1 IFNs, which are important for host defense against viral and pathogenic invasion. This causes various types of Interferon Stimulated Genes (ISG) to be produced. It was hypothesized to see a decrease in type 1 IFN expression when IRF3 was knocked down in macrophages. To determine how the lack of IRF3 in macrophages impact type 1 IFN response, LysM IRF3: Cre positive and Cre negative mice were used as models and tested against various interferon stimulated genes to measure type 1 IFN expression.

Method

LysM IRF3 deficient mice in macrophages were infected with 10,000 PFU of MHV68. The mice were euthanized, and lungs were harvested at 16 dpi. Lungs were kept in TRIzol at -80 C and later lysed for RNA extraction. After RNA was obtained, samples were quantified and prepped for cDNA synthesis. During cDNA synthesis, primers were used to target specific ISGs in order to measure gene expression through a quantitative reverse transcriptase polymerase chain reaction (qRT-PCR).

Results

Results from the qRT-PCR machine show similar levels of type 1 IFN expression among Cre positive and Cre negative lungs of MHV68 infected mice who were IRF3 deficient in macrophages.

Summary & Conclusion

Results from this study demonstrate similarities in the expression of type 1 IFN signaling, Mx1 and MNDA. This suggests that another non-macrophage cell type of IRF3 in the lungs is producing enough type 1 IFN to maintain global signaling during infection. Although significant changes weren't seen in type 1 IFN driven ISG expression (Mx1, MNDA), there was an unexpected decrease in CxCL9 (type 2 IFN driven) induction in Cre pos mice models, which demonstrates an unknown connection between IRF3 induced type 1 IFN and a distinct type 2 IFN system.

Key Words: gammaherpesvirus, macrophages, IRF3, type 1 IFN, interferon stimulated genes

Jacob Zaiser – Lehigh University
Dr. Aoy Mitchell, PhD and Dr. John LaDisa, PhD
MCW Department of Surgery

NPRC Gene Variants in Coarctation of the Aorta and Hypoplastic Left Heart Syndrome

Coarctation of the aorta (CoA) is a congenital cardiovascular disease consisting of a narrowing of the proximal descending thoracic aorta, often resulting in hypertension despite early intervention. Based on recent studies, Natriuretic Peptide Receptor Type-C *(NPRC)* has been shown to be downregulated in proximal regions subjected to higher blood pressure (BP) from CoA versus distal regions subjected to normal BP (*LaDisa et al. Physiol Genomics 2019;51:177-185)*. We hypothesize *NPRC*, a gene associated with higher BP, cellular proliferation, and their molecular mediators, may have an important role in arterial function ultimately resulting in stiffening and hypertension. CoA is commonly associated with other heart malformations and is frequently a component of the anomaly in the majority of patients with HLHS. In this study, whole exome sequencing was performed on 59 CoA subjects and 79 HLHS subjects to identify variants in *NPRC*. Two variants, rs146301345 and rs142228984, were identified on exon 7 and exon 8 respectively. Both variants were determined to be rare, based on gnomAD Allele Frequency, and probably deleterious based on the predictive tools CADD, PHRED, SIFT, and Polyphen. After designing primers and sending the PCR products to Retrogen for confirmatory Sanger sequencing, both variants were confirmed two subjects, one with CoA and one with HLHS. More recently, a new variant rs1173771, distal to the *NPRC* gene, has been identified as a possible candidate of interest to potentially inhibit a gene that upregulates *NPRC* expression. Further research into this variant can possibly be used to understand downregulation of *NPRC* gene expression. These genetic findings in *NPRC* have potential to further aid understanding into long term complications associated with CoA and related congenital cardiovascular disease.

Jacqui Wittmann – Loyola University Chicago
Dr. Curt Sigmund, PhD and Natalia M. Mathieu
MCW Department of Physiology

G-Protein- Vs β-Arrestin- Mediated Signaling Following GPCR Activation

Background

Hypertension is a global health crisis that contributes to many fatal cardiovascular diseases. One of the main systems implicated in blood pressure regulation is the Renin-Angiotensin System (RAS). The AT1R receptor is a GPCR that is activated through ligand, angiotensin II, binding. After GPCR activation, inside the cell, the G protein pathway is activated which generally increases systemic blood pressure. GPCRs also possess another intrinsic mechanism, though β-arrestin recruitment, that desensitizes the GPCR from signaling and therefore terminates G-protein pathway activation. Selective stimulation of the β-arrestin pathway has demonstrated protective cardiovascular effects such as decreasing blood pressure and increasing cardiac contractility. One method to preferentially activate a specific GPCR pathway is through the use of DREADDs (designer receptors exclusively activated by designer drugs) which are mutated receptors that can only be activated by an exogenous ligand.

Method

Two types of plasmids were grown and isolated, one containing a DREADD for the G protein pathway, and the other containing a DREADD for the β-arrestin pathway. Each plasmid was transfected into HEK 293 cells in triplicate. After transfection and incubation, the cells were treated with the exogenous ligand CNO, which stimulated the transfected receptors and activated the corresponding GPCR pathway. The cells were treated with CNO for either 120, 60 or 5 minutes.

Proteins from the samples were extracted and quantified before running a Western Blot assay using the LICOR protocol. The resulting blots were probed for pERK, total ERK, pAkt, and Akt to measure pathway activation and mCherry as a positive control for transfection.

Results

Analysis of the Western Blot membrane indicated cells transfected with the β-arrestin DREADD produced lower, but more stable levels of pERK throughout CNO treatment. Contrastingly, cells transfected with the G-protein DREADD produced higher levels of pERK initially, followed by a rapid decay in ERK activation as the CNO treatment continued.

Conclusion

Preferential stimulation of the β-arrestin pathway results in lower, but more consistent levels of ERK activation compared to activation of the G-protein pathway which promotes a stronger but more transient activation of ERK. The preliminary successful use of DREADDs in vitro to analyze various GPCR pathways supports the hypothesis that chemogenetics could offer new potential in *in-vivo* studies.

Nina Yang – University of Michigan
Ze Zheng, MBBS, PhD
MCW Department of Medicine, Versiti Blood Research Institute

Differential apoB-100 and apo(a) Concentration in ABO Blood Groups

Nina Yang, BS, BS[1,2,3,4], Ziyu Zhang, MD[2], Mark Castleberry, PhD[2], Ze Zhang, MBBS, PhD[2,5]

[1]Summer Program for Undergraduate Research (SPUR), Medical College of Wisconsin; Milwaukee WI, USA
[2]Versiti Blood Research Institute; Milwaukee WI, USA
[3]College of Literature, Science, and the Arts, University of Michigan; Ann Arbor MI, USA
[4]School of Information, University of Michigan; Ann Arbor MI, USA
[5]Department of Medicine, Medical College of Wisconsin; Milwaukee WI, USA

Background: Non-O blood groups (A, B, and AB) are at a higher risk of developing cardiovascular disease when compared to O blood group. Low-density lipoprotein (LDL) cholesterol is a main driver of cardiovascular risk. Multiple clinical reports showed higher LDL-cholesterol levels in people with non-O blood groups. Lp(a), composed of an LDL molecule and an apo(a) glycoprotein chain, is also a risk factor for cardiovascular disease due to its similar structure to LDL. The distribution of apoB and apo(a) levels in different ABO blood groups remains unknown.

Purpose: To evaluate the apoB-100 and apo(a) levels in ABO blood groups.

Methods: The donor population included 269 adults between the ages of 20 and 40 with varying blood groups (A: 104, AB: 9, B: 33, O: 123). The specific number of samples requested per group were representative of the average distribution of blood groups in the United States. Blood was collected in EDTA-containing tubes and plasma was then isolated after centrifugation at 1,500g for 15 minutes. Samples were kept in 4°C for the duration of the experiments.

Results: The preliminary data shows trends that blood group A has the highest average apoB levels, followed by B, O, and AB (97.63 mg/dL, 93.59 mg/dL, 88.62 mg/dL, 77.02 mg/dL respectively, $p = 0.13$, one-way ANOVA). The median apo(a) levels among blood groups was found to very similar between the blood groups (AB: 7.01 mg/dL, A: 6.79 mg/dL, O: 6.08 mg/dL, B: 3.57 mg/dL, $p = 0.5$, one-way ANOVA).

Conclusion: No conclusions can be made on the preliminary data. Future analyses include adjusting for the overrepresentation of females in the donor population and comparing the difference in apoB and apo(a) levels in non-O blood groups to the O blood group. Gender could be a confounding factor skewing results based on the percentage of a certain gender in a blood group. Future experiments also include testing a larger sample size to obtain more information about the population.

Savanna Blair – Carleton College
Aoy Mitchell, PhD
MCW Department of Surgery

Rare *MYH6* and Sarcomere Gene Variants in the Etiology of Hypoplastic Left Heart Syndrome

Background

Hypoplastic left heart syndrome (HLHS) is a rare and severe congenital heart disease (CHD) characterized by hypoplasia of the left ventricle and ascending aorta as well as mitral and aortic valve defects. Infants with HLHS experience compromised blood flow through the left side of the heart, resulting in abnormal respiration and circulation that requires immediate stabilization and surgical intervention. Although surgical outcomes for patients with HLHS have improved significantly, HLHS remains one of the most lethal forms of CHD, as it is responsible for 23% of cardiac-related deaths within the first week of life but constitutes just 2-3% of CHD cases. Though the cause of HLHS is largely unknown, previous studies by the Mitchell Lab and others have implicated rare cardiac sarcomere gene variants in HLHS. In this study, we aim to confirm the presence of rare and predicted damaging α-myosin heavy chain (*MYH6*), filamin C (*FLNC*), and cardiac myosin binding protein C3 (*MYPBC3*) variants in HLHS subjects.

Method

DNA samples from 258 nonsyndromic HLHS pediatric probands were obtained from the CHD Tissue Bank (Children's Wisconsin, Milwaukee, WI). Inclusion criteria for HLHS was defined by atresia or stenosis of the aortic and mitral valve and hypoplasia of the left ventricle and ascending aorta. Whole exome sequencing (WES) was performed at MCW for 179 of the subjects (Cohort 1, consented 1999-2015) and WES libraries were generated using SureSelectXT Human All Exon kit (v4, v5). Sequencing was accomplished using a 100 bp paired-end module (Illumina) and reads were mapped to GRCh37 using Burrows-Wheeler Aligner.

An additional 79 subjects (Cohort 2, consented 2007-2022) were exome sequenced by Marshfield Clinic, and WES libraries were created using Illumina DNA Prep with Enrichment kit. Sequencing was accomplished using a 100 bp paired-end module (Illumina) and reads were mapped to GRCh38.

Rare (Genome Aggregation Database mean allele frequency $< 2 \times 10^{-3}$) and damaging (Scaled Combined Annotation Dependent Deletion PHRED score > 22.5) variants in *MYH6*, *FLNC*, and *MYBPC3* were identified, and PCR primers were designed for each significant variant using NIH Primer BLAST. PCR Products were visualized by 2% agarose gel, cleaned with ExoSap-IT, and variants were confirmed by Sanger Sequencing (Retrogen) and chromatograms were visualized using Benchling Nucleotide Sequencing Software.

Results

Rare and damaging *MYH6* variants were identified in 10.1% of subjects (26/258), *FLNC* variants were detected in 3.1% of subjects (8/258), and *MYBPC3* variants were found in 2.3% of subjects (6/258). *MYH6* variants were previously confirmed. Two *FLNC* and two *MYBPC3* variants from Cohort 2 were successfully confirmed by Sanger Sequencing. Six *FLNC* and four *MYBPC3* variants from Cohort 1 await confirmation.

Conclusion

The etiology of HLHS is complex and exhibits a strong genetic component. The appeared association of rare, predicted damaging *MYH6*, *FLNC*, and *MYPBC3* variants with HLHS suggests that rare sarcomere gene variants contribute causal risk in a significant fraction (>13%) of nonsyndromic HLHS. Early identification of carriers of rare sarcomere variants may be crucial for prenatal diagnosis of HLHS, and such variants should also be followed to monitor risk for cardiac complications, such as cardiomyopathies, and the need for intervention later in life. Ultimately, sarcomere variants may be candidates for a new class of pharmaceutical compounds, including myosin modulators, that could contribute to increased survival and quality of life for HLHS patients.

Aria Stalnaker – University of Central Florida

Chris Kristich, PhD

MCW Department of Microbiology and Immunology

Enterococcus faecalis's Resistance to Cephalosporins Is Affected by Mutations in the CroS Extracellular Domain

Background: *Enterococcus faecalis* is a bacteria that colonizes the gut of humans. When *E. faecalis* spreads to other parts of the body, it can cause life-threatening infections. It is hard to treat these infections because of enterococci's intrinsic property of having resistance to cephalosporins. Cephalosporins impair cross-linking of the bacterial cell wall resulting in bacterial lysis. One of the systems that allows for *E. faecalis* to have resistance to cephalosporins is the CroRS two-component system (TCS) made up of a sensor kinase (CroS) and a response regulator (CroR). Treatment with cephalosporins leads to CroS auto-phosphorylation and subsequent phosphorylation of CroR, resulting in CroR regulation of gene expression, including the *croRS* operon. Based on the predicted structure of CroS, it most closely resembles an intramembrane histidine kinase. Intramembrane histidine kinases (IM-HK) have two transmembrane domains connected by a short extracellular linker (<20 amino acids). However, the predicted extracellular domain of CroS has 30 amino acids and it is unknown whether the extracellular domain of CroS only functions as an extracellular linker or if it has more functions because of the longer extracellular domain. We hypothesize that the longer CroS extracellular domain may allow for a more active role in sensing and responding to cell wall stress.

Methods: To test this hypothesis, we introduced alanine-stretch mutations in the extracellular domain of CroS and analyzed CroRS abundance and activation in the absence and presence of cephalosporins. Separately, we replaced the predicted 30 amino acid CroS extracellular domain with a 30 amino acid flexible linker (GGGGS repeat). We assessed the cephalosporin resistance phenotype for both mutants.

Results: We found that mutations in the extracellular domain of CroS altered cephalosporin resistance compared to wild-type *E. faecalis*. Further, we found that alanine-stretch mutations within the CroS extracellular domain resulted in a decrease in CroS abundance and CroR activation.

Conclusion: These results indicate that the CroS extracellular domain may be important to the CroRS system for more than linking the transmembrane domains of CroS together. Ongoing studies are focused on investigating the other sections of the extracellular domain of CroS by introducing alanine-stretch mutations and by replacing the extracellular domain with a 10 amino acid flexible linker.

Sam Patterson – Washington University in St. Louis
Jennifer Knight, MD, MS, FACLP
Natalie McAndrew, PhD, RN, ACNS-BC, CCRN-K
MCW Department of Psychiatry and Behavioral Medicine

The Experiences of Patients Who Underwent Hematopoietic Stem Cell Transplant During the COVID-19 Pandemic

Background
Hematopoietic stem cell transplantation (HCT) involves aggressive treatment regimens, extended hospitalizations, and a high level of patient engagement in care. During HCT, patients are severely immunocompromised and often endure demoralizing periods of social isolation to prevent infection. Fears about complications such as graft-versus-host-disease (GVHD), toxic side effects, and the potential risk of death can lead to psychological distress. The COVID-19 pandemic presented HCT patients with additional system-related barriers, including limited donor availability, blood supply shortages, and scheduling delays. COVID-19 restrictions increased patient loneliness, placing these already vulnerable patients at a greater risk for increased morbidity and mortality. Undergoing HCT during the height of a pandemic is a unique experience. Therefore, the goal of this study was to describe the patient perspective of HCT during the COVID-19 pandemic.

Method
This is a qualitative, descriptive study. In the parent study, patients were identified through the Center for International Blood and Marrow Transplant Research (CIBMTR) who received a transplant during March through September 2020. A repository of patients willing to be contacted for additional research was created by CIBMTR, and the study PI contacted and recruited 25 participants for a one-on-one interview about their transplant experiences. Interviews were transcribed verbatim by a professional transcription service. Inductive qualitative content analysis was used to determine the manifest and latent themes from patient interviews. Trustworthiness/rigor was established by (1) creating a detailed audit trail of the analytic process, (2) meeting frequently as a study team to discuss findings, and (3) ensuring agreement on analytic steps from initial coding to the development of themes.

Results
We identified four main themes: (1) Transplant is an arduous journey; (2) The COVID-19 pandemic severely complicated the transplant experience; (3) Transplant requires extensive dedication and commitment; and (4) Transplant contributes to personal transformation. Participants described intense physical symptoms, persistent fears of infection, and frustration with prognostic uncertainty. Patients also revealed that COVID-19 introduced severe complications to the transplant experience, such as isolation and loneliness in the hospital without in-person family support, delays in treatment, and a lack of donor availability due to worldwide shutdown. In the survivorship period, patients expressed profound gratitude toward caregivers, lasting emotional trauma, and existential quandary.

Conclusion
Although transplant and the COVID-19 pandemic were extraordinary stressors for HCT patients, many described a new sense of meaning, connection, gratitude, and intention to help others undergoing transplant. Developing tailored supportive interventions for HCT patients and their caregivers throughout the transplant process is a priority direction for research.

Keywords: COVID-19, HCT, Resilience, Existential Distress, Isolation

References

Rueda-Lara, M., & Lopez-Patton, M. R. (2014). Psychiatric and psychosocial challenges in patients undergoing haematopoietic stem cell transplants. *International review of psychiatry (Abingdon, England)*, *26*(1), 74–86. https://doi.org/10.3109/09540261.2013.866075

Amonoo, H. L., Massey, C. N., Freedman, M. E., El-Jawahri, A., Vitagliano, H. L., Pirl, W. F., & Huffman, J. C. (2019). Psychological Considerations in Hematopoietic Stem Cell Transplantation. *Psychosomatics*, *60*(4), 331–342. https://doi.org/10.1016/j.psym.2019.02.004

El Chaer, F., Auletta, J. J., & Chemaly, R. F. (2022). How I treat and prevent COVID-19 in patients with hematologic malignancies and recipients of cellular therapies. *Blood*, *140*(7), 673–684. https://doi.org/10.1182/blood.2022016089

Proxson Cheriyan – University of Wisconsin-Parkside
Jeffrey A. Medin, PhD
MCW Department of Pediatrics

Production and Quantification of Novel Next-Gen Bispecific Antibodies

Hodgkin's Lymphoma (HL) is a prevalent childhood cancer that affects the lymphatic system and has a relative five-year survival rate of 88.9%. Upon relapse, many patients present with refractory HL to traditional small molecule treatments. Immunotherapy has been shown to often be efficacious to refractory HL. One such immunotherapy is the use of bispecific antibodies, which can recognize two different targets. When administered, these bispecific antibodies can trigger an immune response against cancer cells by binding tumor and immune cells closely. A first generation bispecific has been created and characterized. This bispecific antibody consisted of two IgGs chemically conjugated together and was inefficient to manufacture. New bispecific antibodies have been designed, and these second generation bispecifics can be expressed as a single protein chain. Initial studies have shown the antibodies to be functional and efficacious. Further testing will be needed to confirm efficacy, which will require larger quantities of antibodies. The goal of my project was to produce large amounts of the next generation bispecific antibodies, named Clincher and Grappler. Grappler consists of two binding regions connected by flexible linkers and a fragment crystallizable (Fc) region from an IgG antibody. Clincher bispecific antibodies are the third generation bispecific, replacing a flexible linker with a hinge sequence also from an IgG antibody. This allows for binding with several more types of immune cells. These bispecific antibodies can bind to CD3 on T-Cells and CD30 on Hodgkin's Lymphoma (HL) cancer cells. CD3 is a component protein in the T cell receptor complex that is essential for the activation of T-cells, while CD30+ cells are found on cancerous Reed-Sternberg B-cells and are a common tumor marker for HL. The antibodies were produced using suspension Human Embryonic Kidney (HEK) cells using the Expi 293 Expression System. One week post-transfection, Grappler or Clincher antibodies were harvested from the media. These antibodies were purified from the media using Protein A/G affinity chromatography columns. The antibodies were then eluted using citric acid. Antibody concentrations were measured using a Bicinchoninic acid (BCA) assay. The results of the BCA assay showed 17.8 mg of Grappler and 22.7 mg of Clincher were produced through seven transfections. These relatively large amounts of the two will allow for many future experiments to show their potential as HL treatments.

Keywords: Immunotherapy, Cancer, Bispecifics, CD3, CD30

Debbie Stenzel – University of Wisconsin Parkside

Dr. Ryuma Tanaka, MD

MCW Department of Pediatrics

Exploring GD3 Expression on Brain Tumor Cells and Characterizing a Specific CAR T Cell Phenotype

Brain cancer remains the leading cause of cancer-related death among children, emphasizing the critical need for effective treatments. Immunotherapies, including chimeric antigen receptor (CAR) T-cell therapy, represent a promising direction in cancer research by utilizing modified T cells, a type of white blood cell integral to our adaptive immune response, to recognize and eliminate tumor cells expressing specific antigens. My research aims to assess ganglioside D3 (GD3) expression on pediatric brain tumor samples as identifying elevated GD3 expression would indicate the potential suitability of CAR T cell therapy for these tumors. Further, a known barrier to the success of CAR T-cell therapy is T-cell exhaustion which impairs the cell's ability to detect and eliminate cancer cells effectively. The mTOR pathway is involved in driving T-cell exhaustion by promoting metabolic reprogramming and impairing key signaling pathways, allowing the persistence of cancer. My research additionally aims to investigate the impact of varying concentrations of Temsirolimus, an mTOR inhibitor, on alleviating T cell exhaustion. To assess GD3 expression, samples of brain tumor were homogenized, and glycolipids were isolated by organic extraction followed by saponification, desalting on tC18 Sep-Pak chromatography, and a hexane wash. Finally, the samples were permethylated. Mass spectrometry analysis of tumor samples demonstrated the expression of galactosylceramides and gangliosides by displaying peaks at 1371, 1733 and 1978 m/z indicating the expression of GM3, GD3 and GD2 respectively. To investigate T cell exhaustion, human peripheral blood mononuclear cells (PMBCs) were isolated from a blood sample and T-cells were stimulated using CD8/CD28 Dynabeads. CARs were introduced into the T-cells via a lentiviral vector. T-cells were then cultured in a six-well plate, each receiving a concentration of Temsirolimus ranging from 0nM-1μM. To measure T-cell exhaustion, flow cytometry detected fluorescently labeled CD45RA and CCR7 markers on T-cells that allow classification of their subset. Analysis demonstrated that 10nM Temsirolimus promoted a favorable CAR T-cell phenotype, displaying 28% more naïve T-cells compared to untreated T-cells. Naïve T-cells are vital for effective immunotherapy due to their proliferative potential and lack of prior antigen exposure. Higher concentrations (≥50nM) showed no significant further changes. To conclude, identifying GD3 expression on brain tumor samples identifies it as a possible target for CAR T-cell therapy. Moreover, low concentrations of Temsirolimus may reduce T-cell exhaustion, enhancing the effectiveness of CAR T-cell therapy.

Keywords: mTOR pathway, Temsirolimus, mass spectrometry, CAR T-cell therapy

Christian Chang – Baylor University
Yiliang Chen, PhD
Versiti Blood Research Institute

HDL Regulates Lysosome Activity Within Macrophages

Background

Macrophages take up oxidized LDL (oxLDL) to produce lipid-laden foam cells which lead to atherosclerosis development. Foam cell formation can be reduced by macrophage cholesterol efflux mediated by HDL, which transports extra cholesterol to the liver to be excreted. This process requires lysosomal digestion of cholesteryl ester to free cholesterol, before they can be exported to extracellular HDL. Subsequently, expressed on macrophage surfaces is receptor SR-BI which interacts with HDL. While it mediates the bidirectional flux of cholesterol between macrophages and HDL, little is known about the effect of HDL/SR-BI binding on macrophage lysosomal activity. We aim to test the hypothesis that HDL/SR-BI binding increases lysosome activity in macrophages.

Method

Wild type (WT) or SR-BI knockout (KO) peritoneal macrophages were isolated and cultured *in vitro*. The macrophages were plated and were assigned to one of three conditions: control, oxLDL, oxLDL/HDL. Macrophages were treated with 50 μg/ml oxLDL for 24 hours to generate foam cells. Then, oxLDL was replaced with 50 μg/ml of HDL for two hours. After the first hour of HDL treatment, self-quenched substrate was added to all groups for an additional hour. The substrate was digested in the lysosomes, and when intracellular lysosomes were activated, the self-quench group was cleaved and produced fluorescence. Flow cytometry was conducted to measure the substrate fluorescence as an indicator of lysosomal activity. One-way ANOVA was conducted to determine statistical significance.

Results

Compared to control, oxLDL increased lysosomal activity in both WT (p = 0.0158) and SR-BI KO (p = 0.0042). However, after the addition of HDL, lysosome activity reduced compared to oxLDL alone in both WT (p = 0.0292) and SR-BI KO (p = 0.0129).

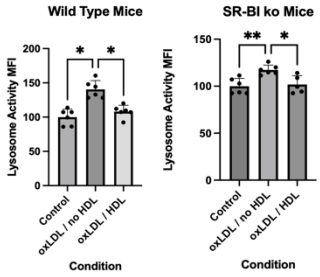

Conclusion

The uptake of oxLDL by macrophages increases the cell's lysosome activity. However, upon stimulation with HDL, these cells reduce their lysosome activity to a level similar to control macrophages. This suggests that HDL may play a role in decreasing lysosome activity. However, this experiment suggests that HDL/SR-BI binding is not the cause of this reduction in lysosomal activity.

Neha Kurpad

Abstract

Introduction: Suicide is a public health issue and suicide rates continue to rise throughout the years. Cultural minorities experience mental health issues and suicidal symptoms in different ways due to their culture. Among South Asian individuals, familial relationships and status within the community are integral to the culture, values that contrast with American cultural values of individuality and independence. South Asian women are at a higher risk for psychological disorders and suicide, because of gender roles that heighten cultural expectations including responsibility for cultural continuity, and the family caretaker role. Understanding the impact of familial relationships on psychological and suicidal symptom risk is valuable, so that prevention can focus on decreasing family discord to improve mental health. Mothers play an integral role in the family, and it has been found in other minority populations that strained relationships with mothers can increase suicide risk. In addition, second-generation immigrants may experience acculturation stress and discord within the family, which are risk factors for suicide.

Study objective: The aim of this study is to use qualitative interviews and thematic analysis to determine if there are particular characteristics of the South Asian mother-daughter relationship that are related to increased risk factors for suicide. We expect to find that themes such as low mutuality, lower engagement, and higher levels of conflict over acculturative factors and cultural norms will be associated with an increased risk of suicidal behaviors.

Mijoo Kim – Concordia University Wisconsin
Lu Han, PhD
MCW Department of Pediatrics

The role of Lmnb2 on centrosome structure in human iPSCs and derived heart muscle cells

Ischemic heart injury and heart failure have become the leading cause of death in the United States (D'Uva et al., 2015). Therapies based on heart muscle cell (cardiomyocyte) proliferation hold a promise to replace the damaged myocardium and improve heart function. However, adult mammalian cardiomyocytes lose their ability to proliferate, which creates the barrier for heart regeneration (Tzahor and Poss, 2017). On the other hand, fetal and neonatal mammalian cardiomyocytes are able to proliferate (Polizzotti et al., 2015). The mechanism of this transition of cardiomyocytes is not clearly found yet. Our lab has found that the level of nuclear lamina filament Lamin B2 (Lmnb2) regulates cardiomyocyte mitosis and myocardial regeneration (Lu et al., 2020). Also, we have observed mitotic block and abnormal spindle formation in Lamin B2 depleted cardiomyocytes (Lu et al., 2020). The mechanism of how Lmnb2 regulates mitosis remains unknown. So, we focused on understanding how Lmnb2 regulates mitotic spindle organization via centrosome in stem cells as well as cardiomyocytes. Centrosomes are composed of centriole and pericentriolar matrix (PCM). Also, centrosomes are the main organelle to organize the mitotic spindle and play an essential role in mitosis. Therefore, this study advances the understanding of how Lmnb2 affects centrosome structure in stem cells and cardiomyocytes. CRISPR/Cas9 genome editing was used to generate Lmnb2 knock-out human induced pluripotent stem cells (iPSC). The Lmnb2 gene inactivation was confirmed by qPCR and Western blot. Human iPSCs were differentiated into cardiomyocytes using WNT signaling pathway modulation in monolayer culture. Centrosome structure was determined by immunofluorescent microscopy of Pericentrin (PCNT), a key component of PCM of centrosomes. DNA synthesis was quantified by EdU labeling. Mitosis was examined by phosphorylated Histone H3 staining. Our results showed that Lamin B2 depletion has no significant effect on DNA synthesis and mitosis in human iPSCs ($p>0.05$, $n=9$). However, Lamin B2 depletion significantly decreased mitosis in cardiomyocytes ($p<0.01$). Lamin B2 depleted iPSCs have no significant difference in centrosome structure compared with wild type ($p>0.05$, $n=9$). In contrast, Lamin B2 depleted cardiomyocytes have significant differences in centrosome structure compared with wild type ($p<0.0001$). In conclusion, the level of Lamin B2 did not change the proliferation and centrosome structure in stem cells, but is essential for the proliferation and centrosome structure in cardiomyocytes.

References

Han, Lu, et al. "Lamin B2 Levels Regulate Polyploidization of Cardiomyocyte Nuclei and Myocardial Regeneration." Developmental Cell, vol. 53, no. 1, 2020, https://doi.org/10.1016/j.devcel.2020.01.030.

D'Uva, Gabriele, et al. "ERBB2 Triggers Mammalian Heart Regeneration by Promoting Cardiomyocyte Dedifferentiation and Proliferation." Nature Cell Biology, vol. 17, no. 5, 2015, pp. 627–638, https://doi.org/10.1038/ncb3149.

Tzahor, Eldad, and Kenneth D. Poss. "Cardiac Regeneration Strategies: Staying Young at Heart." Science, vol. 356, no. 6342, 2017, pp. 1035–1039, https://doi.org/10.1126/science.aam5894.

Polizzotti, Brian D., et al. "Neuregulin Stimulation of Cardiomyocyte Regeneration in Mice and Human Myocardium Reveals a Therapeutic Window." Science Translational Medicine, vol. 7, no. 281, 2015, https://doi.org/10.1126/scitranslmed.aaa5171.

Megan Prahl – University of Wisconsin-Madison
Olena Isaeva, PhD
MCW Department of Cell Biology, Neurobiology, and Anatomy

Effect of chemotherapy treatment on mechanosensitivity of mouse keratinocytes

Background

Chemotherapy-induced peripheral neuropathy (CIPN) is a major adverse side effect of chemotherapy treatment. Paclitaxel is one of the most common chemotherapeutic agents used for treating various forms of cancer, such as lung, ovarian, and breast cancers. Paclitaxel has one of the highest rates of prevalence of CIPN in patients receiving this treatment, underscoring the need to investigate the specific mechanisms by which paclitaxel causes peripheral neuropathy, which remains unknown. Keratinocytes are known to respond to mechanical stimuli and contribute to touch sensation. Our lab has shown that systemic treatment of mice with paclitaxel increases epidermal cells' mechanically evoked calcium response *in vivo*. This study aimed to examine the effect of paclitaxel treatment on the mechanically evoked calcium response in keratinocytes and the propagation of this response to neighboring cells *in vitro*.

Method

Keratinocytes were isolated from mouse glabrous hind paw skin and cultured for three days. On the day of the experiment, cells were loaded with a calcium indicator (Fura-2 AM) for 45 min. Cells were then treated with 1 µM paclitaxel or vehicle for 30 min. Keratinocyte calcium responses were elicited by applying mechanical stimuli using the glass probe with a blunted tip. We evaluated the amplitude of stimulated cells' mechanically evoked calcium response and the propagation of calcium response to neighbor "unstimulated" cells.

Results

Paclitaxel treatment *in vitro* does not affect the amplitude of keratinocytes' calcium response to mechanical stimulation. Moreover, it significantly decreases the number of neighbor cells activated in response to the mechanical stimulation of a single keratinocyte.

Conclusion

The present study shows that treatment of keratinocytes with paclitaxel *in vitro* does not replicate the effect of systemic paclitaxel treatment on epidermal cells' mechanosensitivity *in vivo*, suggesting the complex impact of chemotherapy treatment on keratinocytes sensitivity to mechanical stimulation in *in vivo* settings.

Anna Bauer – St. Norbert College
Michael Zimmermann, PhD
Linda T. and John A. Mellowes Center for Genomic Sciences and Precision Medicine at the Medical College of Wisconsin

Molecular Analysis of CHD7 Variants in Atypical CHARGE Syndrome

Background

Brace for uncharted territory in the realm of rare genetic diseases. Genetic variants are only considered disease-causing when their functional mechanisms are understood. Thus, genetic screening disregards many novel variants, leaving great need for characterization of these new disease mechanisms.

CHARGE Syndrome (CS) is an autosomal dominant complex genetic syndrome, with phenotypes not limited to **c**oloboma, **h**eart anomaly, **a**tresia of the choanae, **r**etardation, and **g**enital and **e**ar anomalies. Since this wide range of symptoms has no clear genetic cause, it is considered a syndrome rather than a disease. This study focuses on characterizing the molecular mechanisms of two novel genetic variants of uncertain clinical significance (VUS) discovered in atypical CS patients at Mayo Clinic. Our primary goal is to compare the VUS from Mayo Clinic to other CS variants and to further annotate their molecular mechanisms.

The protein Chromodomain-Helicase DNA-binding protein 7 (CHD7) is a transcription regulator involved in translocating nucleosomes. Additionally, CHD7 is a major cause of CS as around one third of cases implicate CHD7.

Method

Initially, research on CHD7 and its role as a chromodomain remodeler was conducted to construct an idea of the protein's overall purpose. After reviewing case studies of missense variants and supplementing additional typical and atypical CS variants, all variants were structurally analyzed, emphasizing the use of structural bioinformatics for the ultimate characterization while utilizing autoinhibited and DNA bound models (synthesized with various bioinformatic tools). By piecing together these components to create a story, how to approach each unique mutation with its corresponding unique disease mechanism is better understood.

Results

Side chain replacements S1026Y and V1438G may impact their local environment due to length and hydrophobicity changes, respectively - however further experimentation is needed to measure the extent of damage. Pathogenic comparator variants appear to impact structural stability more than benign comparator variants, while other data suggest VUS impact local energetic sidechain compatibility.

Conclusion

By characterizing the atypical CHARGE variants from Mayo by their disease-causing mechanism, there is insight into the variant. A diagnosis of a rare genetic disease holds great strength in patient care molecularly. By looking at the VUS from Mayo, these classifications have been updated from inferring the disease mechanism via examining and quantifying variants' local environments, energy calculations, and molecular interactions. Along with providing information pertaining to the disease mechanism, further patient diagnosis and treatment improves patient care.

Merub Irfan–Alverno College
Matthew Kudek, M.D
MCW Department of Pediatrics

Allogeneic CD8 T cells deplete host ILC3 in GVHD of the Colon

Graft versus host disease (GVHD) is one of the common life-threatening diseases where the donor's bone marrow or stem cells start reacting against the host causing tissue damage leading to multiorgan failure (Zeiser and Blazar, 2017). Antigen expressing type 3 innate lymphoid cells ($MHCII^+$ ILC3s) are critical for inflammation, protecting the intestinal mucosa, and maintaining gut homeostasis (Zeng et al., 2019) and studies show that mice with GVHD after allo-HSCT (allogeneic hematopoietic stem cell transplant) exhibit a loss of intestinal ILC3s (Hanash, et al., Immunity 2012). The mechanism by which ILC3s are depleted from the intestinal mucosa during GVHD is not yet known. In the present study, we explored how host ILC3s might be targeted by donor CD4+ and CD8+ cells in the gut during GVHD considering their abundant presence in the colon (Geremia and Cárcamo, 2017). The methods involve GVHD induction into a mouse model followed by injection (IP) with 3 doses of either anti-CD4 or anti-CD8 depleting antibody. Analysis of the colons revealed that in GVHD, CD8+ depletion significantly increased the $MHCII^+$ ILC3s retained in the colon compared with control mice or those with CD4+ depletion. In the group of mice with no GVHD, there is a higher percentage of ILC3s. Hence, we identified a CD8+ T cell mediated process is eliminating host ILC3s during GVHD.

Keywords: Graft versus host disease (GVHD), Type 3 innate lymphoid cells, Mice, CD4+ and CD8+.

Firas Al-Ashker– Pennsylvania State University
Dr. Amit Joshi, PhD
MCW Biomedical Engineering

Luminescent Nanoparticles for Biosensing and Bioimaging

Background

Upconverting nanoparticles luminescent markers has become a promising tool for biosensing and bioimaging. This project goes over different iterations of Gd_2O_3-doped core-shell nanoparticles involving molybdate and rare earth metals like Ytterbium, erbium, and gadolinium. The nanoparticles are then coated in silica and gold. The emission properties of the nanoparticles were studied, and TEM and SEM were used to determine the size of the nanoparticles. The aim of this project was to test different methods of synthesizing upconverting luminescent nanoparticles and see which ones were most efficient. Four batches of nanoparticles were synthesized, two batches of gadolinium oxide doped with ytterbium, erbium, and molybdate, and two batches similarly doped excluding molybdate.

Method

The particles were synthesized by adding specific concentrations of gadolinium nitrate, erbium nitrate, and ytterbium nitrate to 200 ml of distilled water and having it heated up and stirred for two hours. Of these batches, two had urea solution dripped into them through a burette during synthesis, and two had urea added at the start of the synthesis process. After synthesis was completed, solutions were centrifuged, washed, calcinated, grinded, and sonicated. Silica and gold solutions were then added to these nanoparticles before they were tested for size and luminosity.

Results

Pre-coating, the nanoparticles underwent testing using a 1550 nm laser, demonstrating pronounced luminance indicative of their successful functionality. Size characterization was performed utilizing a Zetasizer, revealing dimensions within the range of 70-100 nm, with a hydrodynamic size measured at 300-450 nm.

Conclusion

This project successfully explored the synthesis of upconverting luminescent nanoparticles for biosensing and bioimaging. Different iterations of Gd2O3-doped core-shell nanoparticles were studied, and the nanoparticles were coated with silica and gold. The nanoparticles exhibited pronounced luminance under a 1550 nm laser and had uniform sizes ranging from 70-100 nm with a hydrodynamic size of 300-450 nm. These findings offer promising prospects for the efficient use of these nanoparticles in various biomedical applications.

Sophie Shirali – Washington State University
Hernan Rey, PhD
MCW Department of Neurosurgery

Feature extraction for spike sorting using Gaussian mixture models (GMMs)

Background

Patients with epilepsy receive intracranial encephalograms (IEEGs) to identify the seizure focus. In the Rey lab a modified probe is used to include microwires for extracellular recording. Spike sorting, which is a crucial step for neural activity from different neurons, is done by isolating waveforms from the microwire. With each spike epoching at around 2 milliseconds and a 30 KHz sampling rate, clustering techniques using the full 64 dimensions of the waveforms have proven inadequate. This issue necessitates dimensionality reduction in the feature extraction step of spike sorting.

Hypothesis

Gaussian mixture models (GMM) will allow us to identify features that have a multimodal distribution leading to better separability and create a feature space so that the clustering algorithm can effectively isolate the waveforms from neurons.

Method

In this project, we aimed to investigate the feasibility of utilizing Gaussian mixture models (GMM) as a dimensionality reduction technique to analyze neural signals from epilepsy patients. Our primary objective was to compare the performance of GMM with the current method that uses a Lilliefors test to identify deviations from a normal distribution. The current method can identify multimodal distributions as non-gaussians but will also identify as such other unimodal distributions that do not provide good separability. GMMs offer a promising approach by utilizing a mixture of Gaussian distributions to approximate such distributions and effectively identify multimodal features. By selecting those features, we increase the likelihood of creating a feature space that enhances clustering algorithms.

Using MATLAB, we tested the GMM's ability to fit the distribution of wavelet coefficients, assessing its separability with a maximum of eight Gaussian models. We validate our results using real data recorded from patients.

Results

When comparing the proposed method with the current method, we observed that in most cases, both methods selected the same coefficients. However, in 20-40% of the cases, our method selected different coefficients. When we explored those distributions, we identified that the ones selected by the proposed method were indeed associated with distributions that had better separability. At the same time, the ones selected only by the current method were, in general, non-gaussian but had a unimodal distribution. Overall, the associated spaces generated by the proposed method improved cluster separability leading to better isolation of the neural activity.

Conclusion

Our results have indicated that GMMs can improve the identification of multimodal distribution of wavelet coefficients, resulting in a better space for clustering. Future work will include evaluation of a weighted principal component analysis (PCA) to identify redundant dimensions to further reduce the dimensionality of the feature space.

Daniel Deltgen – Wisconsin Lutheran College
Michele Battle, PhD
MCW Department of Cell Biology, Neurobiology, & Anatomy

Impact of GATA4 Knockout on Human Esophageal Cancer Cell Proliferation

Background

Human esophageal cancer histologically presents as esophageal adenocarcinoma (EAC) and esophageal squamous cell carcinoma (ESCC). Esophageal cancer is the 7th leading cause of cancer deaths worldwide and has one of the lowest five-year survival rates compared with other forms of cancer.

The presence and activation of the *GATA4* gene positively correlates with EAC and ESCC development. GATA4 is not expressed in noncancerous esophageal cells. GATA4 can shift a stratified squamous cell phenotype toward a simple columnar cell phenotype.

We explored the impact of GATA4 activity on the proliferation of EAC and ESCC cells in vitro using two EAC cell lines (FLO-1, OE33) and one ESCC cell line (TE-1). We hypothesized that GATA4 knockout in human esophageal cancer will decrease cell proliferation.

Method

We utilized the CRISPR Cas9 gene editing process to disrupt the *GATA4* gene in each cancer cell line. Clones were isolated, sequenced, and expanded. We used western blotting to confirm the appropriate presence or absence of the GATA4 protein in wildtype and *GATA4* knockout (KO) cells. We performed five-day growth curve analysis for each wildtype and clone cell line (n=3), counting the respective clones electronically. Fifth-day cells were spiked with EdU for 1 hour, fixed, and stained with GATA4, EdU, and DAPI fluorescence markers. We used a Nikon Ti2 U microscope with a Nikon Digital Sight color camera and NIS Elements software, and Adobe Photoshop for imaging stains and GraphPad Prism for graphical figures. Control and KO images for each stain were processed identically.

Results

GATA4 protein was efficiently eliminated from Crispr Cas 9 *GATA4* KO lines. Overall, growth curve analysis showed that GATA4 KO in human esophageal cancer cells failed to significantly decrease cellular proliferation. The proportion of proliferating cells, as measured by EdU incorporation, was also unchanged. The ESCC cell line TE-1, however, did show a trend toward decreased proliferation by both growth curve and EdU incorporation.

Conclusion

Our findings indicate that GATA4 knockout in human esophageal cancer does not decrease cellular proliferation. These data do not exclude the possibility that GATA4 controls other aspects of the tumor phenotype. Future studies will include RNA-Sequencing to identify other pathways to explore in relation to GATA4's role in esophageal cancer.

T'onna Ware – Texas Southern University

Dr. Kristen Beyer PhD, MPH, Ms

Institute for Health & Equity

BACKGROUND: Cardiovascular disease and cancer represent the number one and two causes of death in United States. Prior work has established that presence of cardiovascular disease increases cancer risk and accelerated tumor growth, however the effect of the tumor on progression of cardiovascular disease, especially major adverse cardiovascular events (MACE) independent of therapy has not been established. The immune system and innate immunity have been proven to play a key role in pathology of both diseases. Anti-cancer therapy causes tumor lysis resulting in circulating tumor derived particles that can activate various parts of the innate immune system and are sufficient to cause endothelial dysfunction. Endothelial dysfunction, especially in the microcirculation, is the best predictor for MACE but its importance in MACE of cancer patients is poorly understood.

HYPOTHESES: we hypotheses that tumor burden negatively corelates long term development of MACE in cancer patients by activation of the innate immune system triggering endothelial dysfunction

METHOD: To test the clinical relevance of our hypothesis an observation study was conducted from health records of male and female breast cancer patients without metastatic disease that received cardiotoxic therapy. MACE was established via ICD codes. The tumor burden was categorized by size at diagnosis tumors less or equal to 1 cm, more than 1 or equal to 2 cm, more than 2 or less or equal to 5 cm, and any tumor size greater than 5 cm. Logistic regression was used to calculate odds ratios to examine the relationship between different tumor size and the occurrence of a cardiac event (MACE) controlling for age at diagnosis, sex, race, and prior history of co-morbidities such as atrial fibrillation, coronary heart disease, cardiomegaly, cardiomyopathy, heart failure, peripheral arterial disease and stroke and comorbidity diagnoses.

RESULTS: We created two different tables to support our data. Table 1 shows the findings of the demographic and clinical characteristics. Among patients who have no cardiac events, most had tumors between 1 and 2 cm tumor size (85%). In addition, compared to other tumor size categories the patients who had a tumor size of 2 to 5 cm had the largest portion of cardiac events (19%). The diagnosis age had a standard deviation of 57 years for no cardiac event and 66 for patients with a cardiac event. African American BC patients experienced a higher percentage of a risk to a cardiac event than Caucasian BC

patients. In table 2 we compare the analysis to the reference group of a tumor size less or equal to 1 cm. Patients with a tumor size with less than or equal to 1 cm patients with a tumor size of greater than 1 to less than or equal to 2 cm have 42 percent increased odds of a cardiac event. During our findings, we realized as the tumor size increases so does the percentage of the odds ratio.

CONCLUSION: Overall, our source for the observation was conducted by Froedtert Health. Although we found interesting findings, there are larger patient co-horts outside of Milwaukee, WI that need to be performed. In the future, we plan to move to a bigger database. In our data, w e did not collect information on social-demographic factors such as income and lifestyle behaviors which could have influenced the occurrence of cardiac events. We conclude that it is true larger tumors increase the risk of CVD and we plan to conduct more evidence to support this theory.

[Ari Cross – Smith College, Northampton]
[Carissa Tomas, PhD]
[MCW Comprehensive Injury Center – Division of Data Surveillance and Informatics]

Spatial Predictors of Firearm Injury Incidence: A Geospatial Analysis of Trauma Registry Data

Background

Firearm injury is the 4th leading cause of violence-related injury in ages 15 to 44 in the U.S. For Americans, firearm homicide and firearm suicide is also the leading cause of violence-related injury deaths in ages 5 to 65+ years. Firearm injury incidences are not randomly distributed across areas. Geographic information systems can be used to understand the geospatial relationship between two variables at the census block level. It was hypothesized that density of tangible community resource locations (TCRL) could play a role in the density of firearm injury incidence in census block groups as prior research has found that geospatial access to care can be associated with reduced deaths from gun violence.

Method

Froedtert Hospital's Trauma Registry was used to calculate density of firearm injury locations at the census block group level from 2015-2022. Data from the IRS provided non-profit names and addresses of TCRL in Milwaukee County. Criteria for inclusion of TCRLs included those providing health care or social service outreach such as health clinics, community outreach organizations, and childcare entities. A geographically weighted regression (GWR) was performed to explore the relationship between TCRL density and firearm injury density per census block group while controlling for Area Deprivation Index (ADI), a measure of neighborhood disadvantage, along with population and race derived from the U.S. Census. To reduce the risk of multicollinearity within models, only variables representing the population of one race were used within the model.

Results

Between 2015 and 2020, Froedtert Hospital's Trauma Registry recorded 861 incidents of firearm injury within Milwaukee County, and 733 TCRL were compiled from the Internal Revenue Services' open data portal. The proportion of TCRL per census block group did not align well with the population per census block group or firearm injury density per census block group. The GWR yielded results consistent with that of the null hypothesis in many areas. The near north/central part of the county showed that greater proportions of TCRL's was related to lower injury density. However, given the fact that TCRL's and firearm injury densities are not distributed comparably, this negative relationship of TCRL and firearm injury was not displayed in all of the expected areas of the county.

Conclusion

Geospatial mapping showed inconsistencies in the relationship between TCRL locations and population relative to census block group size. Review of the TCRL coefficients was partially consistent with the null hypothesis in most of the county. Few pockets of the county demonstrated results consistent with the alternative hypothesis. This can be attributed to the disproportionately high rates of firearm injuries within these pockets. The addition of predictors within the GWR could improve future models. For further research, it would be meaningful to investigate the reach of TCRL's in an effort to increase efficacy within these organizations.

Keywords

Firearm, Injury, Prevention, Geospatial

Suggested References

Byrne, James P., et al. “Association between Geospatial Access to Care and Firearm Injury Mortality in Philadelphia.” *JAMA Surgery*, vol. 157, no. 10, 2022, p. 942, https://doi.org/10.1001/jamasurg.2022.3677.
Cook, Alan, et al. “Geospatial Characteristics of Non-Motor Vehicle and Assault-Related Trauma Events in Greater Phoenix, Arizona.” *Injury Epidemiology*, vol. 7, no. 1, 2020, https://doi.org/10.1186/s40621-020-00258-x.

Kale Kroenke, Rowan University
Stéphanie Van-Stichelen, PhD
MCW Department of Biochemistry

Placental Drug Efflux Inhibition via Non-Nutritive Sweeteners

Background: Over the past few decades, public consumption of non-nutritive sweeteners (NNS) in the United States has significantly increased. Several studies and previous research in our lab have identified Sucralose and Acesulfame Potassium (AceK), as substrates for P-Glycoprotein (PGP). PGP, along with Breast Cancer Resistance Protein (BCRP) and Multidrug Resistance-associated Protein 2 (MRP2), are all multidrug efflux transporters and are expressed at the fetal-maternal interface during pregnancy. Inhibition of these proteins by substrate compounds can lead to increased fetal drug exposure. We hypothesize that AceK and Sucralose act as competitive inhibitors for PGP, BCRP, and MRP2. This would suggest NNS consumption during pregnancy could lead to health concerns for the fetus.

Methods: Three different cancer cell lines were used as models for our proteins of interest due to their high endogenous levels of expression: HEK-293 (PGP, kidney model), BeWo (BCRP, placenta model), and HepG2 (MRP2, liver model). Cells were exposed to chemotherapy drugs alone (doxorubicin, vinorelbine, or mitoxantrone), NNS alone (AceK or Sucralose), or combined chemotherapy/NNS. Cell viability was assessed after 24h incubation using MTT assay.

Results: Target concentrations for chemotherapeutic/NNS co-treatment were assessed in chemotherapeutic only treatments and based on ranges where linear dose-response decrease in viability was observed. Sucralose treatment alone significantly decreased cell viability in all cell models at physiologically relevant concentrations, whereas AceK exposure at the same levels only significantly decreased viability in HEK-293 cells. Co-treatment in BeWo and HepG2 cells did not significantly impact viability more than chemotherapeutic alone. However, in high-PGP expressing HEK-293 cells, co-treatment of AceK and Sucralose at 750 nM and Doxorubicin at 1 and 10 µM, respectively, significantly decreased viability relative to Doxorubicin alone ($p<0.05$, ordinary two way ANOVA and uncorrected Fisher's LSD with a single pooled variance).

Conclusion: These results show that NNS alone impact cell proliferation. A lack of decreased cell viability in co-treatment conditions relative to chemotherapeutic alone suggests NNS are not competitive inhibitors of BCRP and MRP2. Results in HEK-293 confirm previous work demonstrating AceK and Sucralose inhibition of PGP. Our findings suggest NNS consumption in combination with certain over the counter and prescription drugs during pregnancy may increase fetal exposure to teratogens by inhibiting PGP. However, further investigation into these interactions in a clinical setting is recommended.

Keywords: Non-nutritive sweeteners, Pregnancy, Placenta, Acesulfame Potassium, Sucralose, Multi-drug efflux transporters

Sophia Ho – Trinity College Dublin & Columbia University

Stephanie Olivier-Van Stichelen, PhD

Nathan Zwagerman, MD

MCW Department of Biochemistry

Comparing O-GlcNAc Enzyme Expression in Normal vs. Tumor Tissue in Human Pituitary Gland

Background

About 15% of intercranial tumors comprise of pituitary adenomas. The endocrine and neurologic dysfunction resulting from these tumors vary greatly due to the wide range of hormones that can be released. Their classification is dependent on the cell of origin and the presence or absence of autonomous, specific hormone hypersecretion. *O*-GlcNAc is a post-translational modification covalently bound to serine and or threonine residues of nuclear or cytoplasmic proteins. The dynamic cycling of *O*-GlcNAc on and off substrates in *O*-GlcNAcylation–a reversible, enzymatic, atypical glycosylation–occurs via *O*-linked β-N-acetylglucosamine transferase (OGT) and *O*-linked β-N-acetylglucosaminase (OGA) respectively. Our lab previously studied the impact of the *O*-GlcNAc post-translational modification on the etiology of pituitary adenomas. It was shown that *O*-GlcNAc enzymes were upregulated in pituitary adenomas and were associated with increased proliferative profile *in vitro*. We would like to investigate the potentiality of using *O*-GlcNAc enzyme antibodies as a diagnostic tool in pituitary adenomas. We hypothesize that tumor-embedded human pituitary samples will demonstrate increased expression of OGT and OGA compared to a neighboring normal pituitary tissue.

Methods

To investigate this hypothesis, we tested both immunohistochemistry (IHC) and immunofluorescence (IF) protocols to observe OGT and OGA. We first optimized the antibody type and concentrations in mouse pituitary, then healthy human pituitary gland, and finally tested a tumor-embedded (gonadotropin adenoma) human pituitary sample. All human samples were obtained on deceased patients, consented through the MCW tissue bank. Both IHC and IF process slides were imaged using the EVOS microscope and the Cytation 10 montage mode. A hematoxylin & eosin (H&E) stain was also performed to visualize tissue structure.

Results

We established that the Anti-OGT Abcam antibody (ab177941) was the best in the IHC setting when used at 1:1000 dilution, while the Anti-OGT Sigma-Aldrich antibody (O6264) was best for IF when used at 1:200 dilution. On the other hand, we established that the Anti-OGA Abcam antibody (ab124807) was the best in the IHC setting when used at 1:100 dilution, while the Anti-OGA Sigma-Aldrich antibody (HPA076501) was best for IF when used at 1:200 dilution. This was validated both for mouse and human pituitary tissues. When testing our optimized protocol in the post-mortem tumor embedded pituitary sample, we observed that the tumor portions were heavily stained compared to the neighboring healthy tissues. Compared to the IHC images, we saw little to no visible difference in the IF images between the tumor and the healthy tissue.

Conclusion

As previously hypothesized, we confirmed that OGT and OGA were overexpressed in pituitary tumors compared to healthy neighboring tissues. We have also characterized antibodies that could be used in the future to better characterize these tumors. It was determined that IF is not suitable for our application. The results of this study can be used as a pathological assessment in the clinic to diagnose patients. Future steps involve staining different subtypes of pituitary adenomas and comparing their levels of OGT and OGA expression.

Kyle Harkin – University of Wisconsin-Madison
Astrid Stucke, MD
MCW Department of Anesthesia

Looking for Endogenous Opioid Receptor Activation in the Medullary Raphe in Young Rabbits

Background

In adult rabbits, respiratory depression from exogenous opioids is partially mediated by the preBötzinger Complex and Parabrachial Nucleus/Kölliker-Fuse complex in the brainstem. Control experiments also showed endogenous opioid receptor activation in the caudal medullary raphe. The current pilot study investigated the approximate location of the Caudal Medullary Raphe in young rabbits and whether endogenous opioid receptor activation could be found already in immature animals.

Method

The study was approved by the local Animal Care Committee and conformed to NIH standards. New Zealand White rabbits of either sex, age 2-4 weeks (300-600g) were anesthetized, tracheotomized, ventilated, decerebrated, and vagotomized. Phrenic nerve activity was recorded, time averaged and used to calculate respiratory rate and peak phrenic activity (fictive tidal volume). Mechanical ventilation maintained hyperoxic hypercapnia (FiO_2 0.6, $etCO_2$ 50mmHg). We functionally identified the preBötzinger Complex with gridwise local AMPA microinjections (5µl). Local naloxone microinjections (1mM, 50µl each) were placed into the midline raphe at 1.5 and 3mm depth in 0.5mm rostro-caudal steps between 1.5 mm caudal and 1.5 mm rostral of the preBötzinger Complex level. At the end of the experiment, we injected Chicago Sky Blue (50µl) into the caudal end and rostral end of the raphe injection and preBötzinger Complex for postmortem histologic confirmation. Animals were euthanized with intravenous KCl, and the brainstem was removed and fixed with paraformaldehyde 4%. Brainstems were sliced 25 µm thick and were alternatingly left unstained (to identify the blue marker) or dyed with Neutral Red (to identify the local neuron populations).

Results

In 8 rabbits, naloxone injections into the raphe incrementally increased respiratory rate from 29+/- 9 to 36 +/- 17 BPM ($p=0.016$). Peak Phrenic Amplitude increased by 20 (range 1-34)%, ($p= 0.029$). The histology indicated that the caudal end of the raphe injections was on average 1.4 +/- 0.7 mm caudal to obex. The preBötzinger Complex was on average 1.2 +/- 0.9 mm rostral to obex. The rostral end of the raphe injection was on average 2.5 +/- 0.8 mm rostral to obex. In preBötzinger Complex slices, the presence of the N. hypoglossus was similar to adults, but the N. ambiguus was not consistently found. The rostral end of raphe injection coincided with the caudal end of the N. facialis.

Conclusion

Naloxone injections into the medullary raphe resulted in an increase in respiratory rate and peak phrenic activity in young rabbits. The magnitude of the effect was smaller than previously observed in adults. This may suggest that there is less endogenous opioid receptor activation in young rabbits at baseline. Alternatively, the contribution of the medullary raphe to respiratory rate may be smaller in young animals. The histology showed that injections started caudal and rostral to the target area, so there was sufficient coverage of the entire medullary raphe area.

Parabrachial Nucleus/ Kölliker-Fuse complex, preBötzinger Complex, Caudal Medullary Raphe, opioid-induced respiratory depression, respiratory rate control

Mya Suneja – University of Wisconsin-Madison
Allison D. Ebert, PhD
MCW Department of Cell Biology, Neurobiology, and Anatomy

Treatment of astrocyte-mediated pathology in spinal muscular atrophy

Background

Spinal muscular atrophy (SMA) is a pediatric neurodegenerative disease characterized by the loss of motor neurons in the spinal cord. SMA is an autosomal recessive disease caused by a lack of the survival of motor neuron, or SMN1, gene, and often results in respiratory issues, muscle weakness and atrophy, and death. However, restoring SMN1 to motor neurons alone is not a sufficient treatment for SMA; glial cells play a supporting role in motor neuron survival and function and may mediate SMA pathology and progression.

Astrocyte-mediated microglial activation has been shown to increase neuroinflammation through cascades involving pro-inflammatory cytokines. We hypothesized that targeting an overexpression of IL-1ra and a knockdown of CCL5 may reduce astrocytic activation and neuroinflammation, and we hypothesized that reducing astrocytic activation may decrease the presence of Complement Component 3 (C3) present on motor neurons.

Methods

The SMNΔ7 mouse model of SMA was utilized to examine our hypothesis *in vivo*. Treatment was injected into the lateral ventricle of the brain with either a control or experimental adeno-associated virus on day two of life. The experimental virus used the astrocyte promotor GFAP and an mCherry tag to drive IL-1ra expression and shRNA knockdown of CCL5. The control virus expressed mCherry and a scrambled shRNA. Each day, "time to right" behavioral assays were performed, and weight was recorded. Brain and spinal cord samples were then collected and analyzed by western blot, enzyme-linked immunosorbent assay (ELISA), and immunohistochemistry.

Results

ELISA displayed increased IL-1ra cytokine expression and decreased CCL-5 cytokine expression for brain and spinal cord samples that received our experimental virus compared to the control virus. In addition, both western blot analysis and immunohistochemistry displayed decreased amounts of C3 expression in samples receiving the experimental virus injection compared to those which received the control virus injection, but other markers of glial activation were less effected. Functionally, SMNΔ7 mice treated with the experimental virus showed a small but significant increase in lifespan and motor function compared to control virus treated mice.

Conclusion

Overall, we conclude that an astrocyte-targeted IL-1ra overexpression and CCL-5 knockdown may result in decreased neuroinflammatory cascades, reduced astrocytic activation, and improved motor function in the SMNΔ7 mouse model. In addition, these decreased neuroinflammatory cascades may decrease C3 expression and overall motor neuron loss. These findings may further advance treatment options for spinal muscular atrophy patients by lengthening lifespan, lessening symptoms, and improving overall motor function.

Joel Pan – University of Wisconsin - Madison
Dr. Alison Kriegel, PhD
MCW Department of Physiology

Effects of Time-Restricted Feeding on Salt-Sensitive Hypertension: An Echocardiographic Analysis

Background

Hypertension, a prevalent cardiovascular disorder worldwide, is a major risk factor for various cardiovascular diseases, including heart failure.[1] Salt-sensitive hypertension is characterized by an increased sensitivity to dietary salt intake, leading to exacerbated blood pressure fluctuations and adverse cardiovascular outcomes.[2] The pathophysiology of salt-sensitive hypertension involves complex interactions between genetic, environmental, and dietary factors, making it a challenging condition to manage effectively. This research project aims to investigate the potential benefits of time-restricted feeding (TRF) and different levels of dietary salt on salt-sensitive (SS) hypertensive rats. TRF involves limiting food consumption to specific time windows, which has shown promising results in mitigating various metabolic disorders.[3] In this study, we hypothesize that implementing TRF will ameliorate the adverse effects of salt-sensitive hypertension.

Method

Four groups were examined in this study: LS ad lib (low-salt ad libitum), LS TRF (low-salt time-restricted feeding), HS ad lib (high-salt ad libitum), and HS TRF (high-salt time-restricted feeding). Male SS rats (n=7-9/group) and female SS rats (n=4/group) were randomly assigned to these groups at 9-10 weeks of age. The LS diet, containing 0.4% NaCl (AIN-76A; Dyets Inc.), served as the control diet, while the HS diet, containing 4.0% NaCl (AIN-76A; Dyets Inc.), represented high-salt intake. During the first week, all animals had ad lib access to their respective diets to establish hypertension in the HS groups. TRF was implemented during the second week, with an 8-hour feeding window (22:00-06:00) provided during the active cycle. At the end of the second week, echocardiography and blood pressure measurements via carotid artery catheterization were performed in anesthetized rats to assess cardiac structure and function. The echocardiographic data will be analyzed to determine left ventricular dimensions, ejection fraction (EF), fractional shortening (FS), and other relevant cardiac parameters. To assess the effects of time-restricted feeding and dietary salt levels on the echocardiographic parameters, a two-way ANOVA with multiple comparisons ($p<0.05$) using the Tukey method was conducted.

Results

The echocardiographic data indicates that there are variations in left ventricular posterior wall dimensions (LVPWd/LVPWs) and interventricular septal dimensions (IVSd/IVSs) among the experimental groups of salt-sensitive male and female rats. While some trends suggest potential differences, the small sample sizes limit the statistical significance of these observations. The EF and FS values of both the male and female groups consistently showed a non-significant trend of improvement in the TRF groups compared to the ad libitum groups, with the HS TRF group demonstrating the most enhancement in cardiac function.

Conclusion

TRF shows potential effects on left ventricular dimensions in SS hypertensive rats, indicating trends in cardiac remodeling, with possible improvements in both ejection fraction (EF) and fractional shortening (FS) in the HS TRF feeding group, however, future studies are required to better understand these findings.

Keywords: time-restricted feeding, salt-sensitive hypertension, echocardiography, cardiovascular diseases, dietary salt intake

References

1. Fuchs, F. D., & Whelton, P. K. (2020). High blood pressure and cardiovascular disease. Hypertension, 75(2), 285–292. https://doi.org/10.1161/hypertensionaha.119.14240
2. Majid, D. S. A., Prieto, M. C., & Navar, L. G. (2015). Salt-sensitive hypertension: Perspectives on intrarenal mechanisms. Current Hypertension Reviews, 11(1), 38–48. https://doi.org/10.2174/1573402111666150530203858

3. Boyd, P., O'Connor, S. G., Heckman-Stoddard, B. M., & Sauter, E. R. (2022). Time-restricted feeding studies and possible human benefit. JNCI Cancer Spectrum, 6(3). https://doi.org/10.1093/jncics/pkac032

Khadijah Dhoondia – University of Wisconsin Madison
Sritejasvinthi Karimikonda; Nita Salzman, MD, PhD
MCW Department of Microbiology and Immunology Department of Pediatrics

---

Fibroblast mediated inflammation in enteric bacterial infection accompanied by skin injury

Background

Chronic inflammation of the gut is commonly associated with skin conditions, and many skin diseases are accompanied by an altered gut microbiome. While communication exists between the skin and gut, the underlying mechanisms are poorly understood. A previous study of dextran sodium sulfate mediated colitis in mice determined that disease severity worsens when intestinal inflammation is accompanied by skin injury. Hyaluronic acid (HA) is a key mediator in facilitating this response due to its interaction with fibroblasts. Fibroblasts are spindle-shaped mesenchymal cells known for their role in extracellular matrix (ECM) construction and remodeling. Fibroblasts are also involved in other functions, including immune regulation, inflammation, tissue homeostasis, and fibrosis. Due to the heterogeneity of fibroblast subsets within and across tissues, the impact of skin-gut communication on intestinal fibroblasts in the context of other types of gut injury is unclear. ***We hypothesize that in the context of enteric bacterial infection, skin injury exacerbates fibroblast-mediated inflammation in the cecum***.

Method

We employed a model in which mice were administered a skin injury prior to induction of Salmonella enteritis, using a mutant strain, *ΔaroA*, of *Salmonella enterica* serovar Typhimurium. Fibroblast associated gene expression in response to *Salmonella* was evaluated in cecal tissue using reverse transcriptase quantitative polymerase chain reaction (RT-qPCR).

Results

When compared to *Salmonella* alone, our results demonstrated downregulation of *Vim* (vimentin) expression when infection was accompanied by skin wounding. We also observed increased expression of *Fn1* (fibronectin) and decreased expression of antimicrobial peptide, *Retlnβ* (resistin like beta), when infection was accompanied by skin wounding.

Conclusion

Vimentin is known to be involved in extracellular matrix (ECM) remodeling. Since the addition of skin wounding downregulates *Vim* expression, this may limit fibroblast capacity to engage in ECM remodeling, allowing inflammation to persist. Prior studies found that fibronectin upregulates interleukin 8 secretion, a proinflammatory chemokine. Upregulation of *Fn1* suggests an increased presence of immune cells to the infected tissue, leading to persistent inflammation. Further, decreased expression of *Retlnβ*, an antimicrobial peptide, can be associated with enhanced susceptibility to infection. Taken together, we suspect that skin injury exacerbates inflammation associated with enteric bacterial infection, likely via HA interaction with cecal fibroblasts. Future studies can validate these results through protein expression analyses and explore the role of HA in this phenomenon. Overall, this study supports that skin wounding exacerbates fibroblast-mediated inflammation. These findings may inform future research investigating the mechanisms of skin-gut communication in health and disease.

Vishnu Guda – Carleton College

Dr. John Mantsch, PhD

MCW Department of Pharmacology and Toxicology

The Effects of Increased Adolescent Endocannabinoid Levels on Adult Anxiety-Related and Social Behaviors

The endocannabinoid system produces necessary feedback to mediate adaptive responses to stressors. In response to stressful stimuli, endocannabinoids are released and bind to cannabinoid receptors on synaptic terminals and dampen stress-related signaling, forming a negative feedback loop. While the endocannabinoid system plays a critical role in moderating stress responses, if the system is persistently activated by chronic stress, particularly in adolescence when the brain is still developing, there is danger of interrupting critical maturation of neuronal circuits. This may increase the risk in adulthood of anxiety-related disorders, antisocial behavior, and substance misuse. The two primary endocannabinoids in the brain are anandamide (AEA) and 2-arachidonoylglycerol (2-AG). The goal of this experiment is to better ascertain the effects of chronically elevating AEA or 2-AG during adolescence on anxiety-related, social, and drug seeking behaviors in adult rats. Adolescent male Sprague Dawley rats were given daily intraperitoneal injections of either JZL184 (JZL;10 mg/kg), URB597 (URB; 0.4 mg/kg), or vehicle from PND 30-40. JZL is a compound which inhibits the activity of the enzyme monoacylglycerol lipase (MAGL), which catabolizes 2-AG, thereby increasing 2-AG levels. URB inhibits the enzyme, fatty acid amide hydrolase (FAAH), which catabolizes AEA, thus increasing AEA levels. Four hours after the last JZL 184, URB 597, or vehicle injection, play behavior upon exposure to an age-matched peer during a 10-minute period and behavior over a 10-minute period on the elevated plus maze (EPM) were assessed. Later, during adulthood, rats were tested at PND 65 for social preference (3-chamber social test) and anxiety-related behaviors measured in an open field. Thereafter, rats undergo surgical implantation of a venous catheter, and are tested for intravenous cocaine self-administration and reinstatement. During adolescence, we observed trends in the effects of JZL and URB on behavior on the EPM. JZL-and URB-treated groups tended to be less active on the open arms of the EPM compared to vehicle-treated controls, suggesting potential anxiety-related effects. Effects on play behavior are currently being analyzed. During adulthood, group differences in open field behavior were not evident. However, in contrast to vehicle controls, rats treated with JZL or URB during adolescence failed to display preference for peer rat in the 3-chamber social preference test relative to a novel object, reflecting potential effects of elevating endocannabinoids during adolescence on adult socialization. Studies examining the effects of adolescent JZL and URB on adult cocaine self-administration and cocaine seeking are ongoing. In conclusion, the data we gathered indicates that despite anxiety-related behaviors not continuing into adulthood, there may be significant anti-social behavior in mature rats which had increased endocannabinoid levels during adolescence.

Juliana Tovar – University of North Carolina at Chapel Hill
Constanza Garcia Keller, PhD
MCW Department of Pharmacology and Toxicology

The Role of Microglia in Acute Stress and Addiction in the NAcore

Background:

With rising concerns regarding substance use disorders (SUDs), many studies have set out to see how stress can lead to an increased vulnerability to addiction. The brain's reward and motivation pathways interact in the same structure in the brain, forming a circuit. Based on previous literature, we have seen that stress "primes" the reward and motivation circuit, and we hypothesize that these changes facilitate the transition to addiction. Our experiments have focused on the Nucleus Accumbens Core, a region of the brain that is involved in the regulation of motivation, reward, and reinforcement. Based on our results, we have seen how stress leads to long lasting changes in the cells and proteins that make up the NAcore: astrocytes, neurons, and the extracellular matrix (ECM). However, we want to know more about the role of microglia in inducing vulnerability to addiction after acute stress exposure. We chose to explore the role of microglia since these cells exhibit glucocorticoid receptors. Within fifteen minutes of stress exposure, we saw a peak in cortisol levels, a hormone that travels back to the brain and can bind to the GR receptors in the microglia, forming a link between stress response and microglia.

Method

For our experiment, 12 male rats were randomly assigned to a sham or stress group. Sham rats remained in home cages for 30 minutes. Stress rats were placed in acrylic flat bottom restraints for 30 minutes. Immediately after the stress or sham conditions were completed rats were sacrificed and perfused, and all brains were collected and preserved. NAcore tissue was sliced, and cells were labeled using the Iba-1 antibody, which can be used as a marker for microglia activation given that it is a microglia/macrophage specific calcium-binding protein. Confocal data sets of microglia morphology were acquired using a Leica SP8 laser-scanning confocal microscope. Images were analyzed using CellSelect-3D Morph software.

Results

Results demonstrate a decrease in microglia Iba-1 fluorescence following acute stress exposure. Image analysis showed a decrease in microglia cell territory, volume, and ramification index. A decrease in ramification index for the stress group implies that cell territory decreased at a larger rate than cell volume. This could indicate that the microglia are transitioning to a more ameboid state, which may further indicate microglia activation.

Conclusion

Results imply that acute stress exposure can lead to changes in microglia morphology that are indicative of an increase in microglia activation. Future research can focus on understanding what occurs as a result of microglial activation. Preliminary research has shown that microglia interact with MMPs, matrix metalloproteinases, which are enzymes responsible for the remodeling and degradation of the extracellular matrix. Future research can also be used to determine how microglia affect or interact with these proteins.

Avina Elangovan – Saint Louis University
Dr. Ramani Ramchandran, PhD
MCW Department of Pediatrics

The Effect of Mutant SNRK Injection and Cyclopamine Treatment on Zebrafish Embryos: A Study on the Relationship between Sonic Hedgehog Signaling and SNRK

Sucrose nonfermenting 1-related kinase (SNRK) gene is a protein that is expressed in various tissues and cell types. A P388L mutation was identified in SNRK in patients diagnosed with Bardet-Biedel Syndrome (BBS), a rare ciliopathy causing symptoms such as retinal degeneration and polydactyly. In the lab's previous work, the BBS P388L mutant SNRK mRNA injection in zebrafish embryos created eye phenotypes, curved tails, and bleeding. Since the sonic hedgehog pathway is involved in eye development, we decided to investigate the interaction between the sonic hedgehog signaling and mutant SNRK.

I aimed to investigate the effect of cyclopamine, a sonic hedgehog inhibitor, on the phenotypes that are a consequence of the mutant SNRK RNA injection in zebrafish embryo. The expected outcomes of our experiment were the exacerbation or rescue of the various phenotypes when the mutant SNRK-injected embryos were treated with cyclopamine. I hypothesized that if we treated mutant SNRK-injected embryos with cyclopamine then the phenotypes would be exacerbated.

To test this hypothesis, a cyclopamine dose-response experiment was first performed to determine the optimal dosage for the zebrafish, which was found to be 50 uM. To study the interaction between mutant SNRK and cyclopamine, around 50 embryos each were injected with either P388L mutant SNRK RNA or control plasmid. Each of these groups was then divided into two, one-half of the embryos were treated with 50 uM cyclopamine and the other half were treated with ethanol. To perform this experiment, we set up zebrafish crosses, collected embryos, injected the embryos at the 1-cell stage, and treated them with cyclopamine or ethanol at 5.5 hours post fertilization. Observations and data collection were then carried out 48 hours post-fertilization to quantify the number of surviving embryos and identify any phenotypic changes. The quantification was done using a microscope and put into an Excel spreadsheet. The entire experiment was replicated another two times, yielding a total of three trials.

The results indicate that, on average, there were fewer eye phenotypes, curved tails, and bleeding in the cyclopamine-treated P388L mutant SNRK mRNA-injected embryos than in the cyclopamine-treated control plasmid embryos. In other words, the mutant SNRK RNA injection rescued the phenotypes produced by cyclopamine treatment. This result suggests that the mutant SNRK RNA rescues the inhibition of sonic hedgehog signaling.

This study provides insights into the relationship between sonic hedgehog signaling and the mutant SNRK. Further research needs to be done to draw conclusive results.

Keywords: cyclopamine, sonic hedgehog signaling, mutant SNRK gene, zebrafish

Selina Yuri Kim – Cornell University
Mentor: Dr. Ankan Gupta Preceptor Host Labs: Ramani Ramchandran, PhD and Kevin Rarick, PhD
MCW Department of Pediatrics

Cilia Proteins as Biomarkers of Traumatic Brain Injury: An *In Vitro* Model System

Background

Traumatic Brain Injury (TBI) is a form of acquired brain damage due to external forces that may result in neurological deficits and alter brain functions. Studies have shown that a forceful impact to the brain can cause damage to blood vessels due to physical deformation and altered blood flow. Endothelial cells line the vasculature and contain an organelle called cilia, which projects from the surface to the lumen of the vessels and acts as sensors of the blood flow. An altered or low blood flow due to a TBI can cause secondary metabolic stress conditions and create an environment with low oxygen (hypoxia) and low glucose (hypoglycemia). Metabolic stress can cause the endothelial cells to lose cilia, which may be detected in body fluids and be a potential biomarker for pathological conditions. The purpose of this study is to model post-TBI metabolic stress in an *in vitro* system using cell culture and to investigate the effects of such secondary metabolic stress on endothelial cilia. We hypothesize that when exposed to hypoxic condition, ECs lose cilia and subsequently ciliary proteins such as Arl13b and IFT88 will show a decreased cellular expression and can be detected in the cell culture supernatants.

Method

To investigate the consequences of secondary metabolic stress post-TBI, endothelial cells cultured in EC medium (Promocell, cat# 22010) or DMEM were exposed to hypoxic conditions in 2% oxygen for 3 hours. Subsequently, ciliary proteins in the culture supernatants were quantified by Western Blots, and cells were analyzed for cilia or ciliary proteins respectively by immunofluorescence (IF) or by Flow Cytometry.

Results

Using Flow Cytometry, we observed lower median fluorescent intensity (MFI) of endothelial cilia proteins Arl13b and IFT88 post-hypoxia. In our IF study, we also observed loss of cilia structure from EC post hypoxia. Consistent to this, western blot data shows that both ciliary proteins Arl13b and IFT88 show a significant increase in the culture supernatants after being exposed to hypoxia.

Conclusion

TBI associated metabolic stress causes endothelial cells to lose cilia and consistently ciliary proteins are quantifiable in culture supernatant. A better understanding of the consequences of secondary metabolic stresses can be established with incubating cells in a longer duration of metabolic stress, and in a combination of various stress conditions. Our next step is to track the loss of ciliary proteins *in vivo*.

Yushin Kim – Concordia University Wisconsin
Brian Volkman, PhD
MCW Department of Biochemistry

Metric-guided Modeling of the Chemokine Receptor Network

Background

Chemokine receptors (CKR) comprise a subfamily of membrane proteins called G-Protein Coupled Receptors (GPCRs) and play a crucial role in the immune response by mediating cellular migration and signal transduction upon interaction with their cognate chemokines. However, the inherent structural complexity of CKRs poses obstacles in structure determination, hindering functional studies necessary for targeted therapies against various immune disorders.

In this project, we utilized the advances in molecular modeling to generate models of chemokine-CKR complexes. Furthermore, based on the empirical knowledge of the chemokine network, a metric system was developed to identify models of falsely paired chemokine and CKR. The end goal of the project is creating a chemokine-CKR complex structure database while potentially identifying previously unknown chemokine-CKR pairs predicted by physically plausible models of those interactions.

Method

AlphaFold was used to model chemokine-CKR complexes with input protein sequences acquired from Uniprot. Then, 24 chemokine-CKR complex structures were generated combining four CKRs (CXCR3, 4, 5 and ACKR3) with six chemokines (CXCL 4, 9, 10, 11, 12, and 13) in a 4×6 matrix. Molecular dynamics (MD) simulations and structural analysis of the models were done using GROMACS and PyMol packages. To assess the accuracy of the models, the ACKR3-CXCL12 complex model was evaluated using the experimental structure (PDB: 7SK5) as a reference.

Results

AlphaFold was able to generate models of all chosen chemokine-CKR complexes, appropriately capturing the key tertiary structures and the binding topologies. Especially, the ACKR3-CXCL12 complex model highly resembled the experimental structure (PDB: 7SK5) with an all-atom RMSD of 2.6Å. However, given that each CKR binds only to its cognate ligands (a subset of the six chemokines), the successful modeling of all chemokine-CKR pairs clearly demonstrates the algorithm's ability to propose unsubstantiated structures.

To distinguish such false models, confidence scores from AlphaFold were examined in addition to the interface interaction energies calculated via GROMACS. The combined application of three scores - predicted interface template modeling score (ipTM), predicted local distance difference test (pLDDT) of interface residues, and interaction energy between interface residues – successfully eliminated all the false models of chemokine-CKR complex with cutoff scores of 0.694, 64.48, and -2020.67 kJ/mol respectively.

Conclusion

We established a chemokine-CKR complex modeling pipeline capable of identifying falsely paired chemokine and CKR. Moving forward, the pipeline will be streamlined to expand this chemokine network database while potentially discovering novel chemokine-CKR pairs.

Keywords: Chemokine, Chemokine Receptor, Structure, GPCR, AlphaFold

Carlos Herrada – Saint Norbert College
John Corbett, PhD
MCW Department of Biochemistry

Elucidating the role of nitric oxide in the attenuation of EMCV replication

Background

Insulin, an essential hormone that regulates glucose levels in the body, is secreted by β-cells within the pancreatic islet. Type 1 diabetes (T1D) is an autoimmune disease in which β-cells are selectively destroyed by an immune mediated reaction. Environmental factors and genetic susceptibility contribute to disease induction. Viral infection is one environmental factor that has been proposed to induce autoimmune killing of β-cells. Viruses in the picornavirus family have been associated with T1D development and the mechanisms of disease induction are associated with islet inflammation and inflammatory cytokine production. The inducible isoform of nitric oxide synthase is one gene that is induced by cytokines in β-cells and is responsible for the production of nitric oxide. This free radical inhibits β-cell function and decreases β-cell viability, potentially contributing to the development of T1D. In contrast to these previous studies, our laboratory has shown that nitric oxide inhibits virus replication in a β-cell-selective manner. My project focuses on examining the mechanisms by which nitric oxide attenuates viral replication.

Method

The encephalomyocarditis virus (EMCV) is a mouse-tropic member of the picornavirus family that induces autoimmune diabetes in mice in a strain-dependent manner. We hypothesize that nitric oxide attenuates EMCV replication by inhibiting phosphatidylinositol-4-kinase (PI4K). PI4K produces PI4P, which functions as a lipid that is essential for EMCV replication. In support of this hypothesis, PI4K is a member of the PIKK family of kinases, and our laboratory has shown that nitric oxide is an effective inhibitor of PI3K. To test our hypothesis, we will investigate how nitric oxide affects PI4P accumulation in the mouse MIN6 insulinoma cells. The primary methods used are RT-qPCR, western blot analysis, and immunofluorescence to monitor amounts of PI4K mRNA, PI4K protein, and PI4P accumulation, respectively.

Results

Preliminary results suggest that there is no significant change in the accumulation of PI4K mRNA or protein in response to increasing concentrations of nitric oxide during EMCV infection. However, preliminary immunofluorescence data suggests that nitric oxide, in a concentration-dependent manner, decreases the amount of PI4P (PI4K product) present on intracellular membranes following EMCV infection.

Conclusion

These preliminary results suggest that nitric oxide may inhibit the activity of PI4K, rather than the amount of PI4K mRNA or protein present. This would account for the suggested decrease of PI4P even though PI4K mRNA and protein levels do not change.

Analise Segarra – Marquette University
Dr. Elizabeth Sweeny, PhD
MCW Department of Biochemistry

Proteasomal degradation of NOX5

Background

NADPH oxidases are a family of 7 enzymes that produce reactive oxygen species (ROS), which is an umbrella term for reactive molecules that are related to increased oxidative stress. Since they are so crucial to the human body and its function, these ROS must be meticulously regulated; as such, disease, cell dysfunction, and death can be a result of increased oxidative stress. Oxidatively modified proteins can either be reduced or degraded using several different cellular mechanisms such as antioxidant proteins. Another one of these mechanisms is known as the proteasome which breaks down proteins to maintain proteostasis. NADPH oxidase 5 (NOX5) produces a superoxide burst in the presence of calcium. Through previous mass spectrometry analysis in the Sweeny Lab, it is suspected that NOX5 has some effect on mediating oxidate modification, thus decreasing proteasomal activity. It is also known that NOX5 can be a target of proteasomal degradation but whether the activation of a NOX5 superoxide burst affects its own degradation is unknown. We hypothesized that the activation of NOX5 enacts its own degradation by the proteasome. We aim to discover the manner in which NOX5 is degraded by the proteasome and whether the presence of a superoxide burst changes its course of degradation.

Method

In order to measure how NOX5 was degraded by the proteasome, all of the groups of human embryonic kidney cells (HEK) that stably produce NOX5 were plated at equal densities and treated with cycloheximide to block protein translation. As a control, dimethyl sulfoxide (DMSO) was used to allow the proteasome to function normally. while one experimental group was treated with proteasome inhibitor MG132 and the other with Bortezomib, a well-known chemotherapy drug that also inhibits the proteasome. Cells were lysed at 5-hour increments to measure NOX5 concentrations through Western Blots to quantify the amount of NOX5 present. A second experiment was done to measure how NOX5 is degraded after a superoxide burst at 1, 5, and 24 hours. The same treatment was given but was treated with ionomycin calcium salt, a chemical that rapidly increases calcium influx. We also stripped the Western Blots and probed for p53, a substrate that is also degraded by the proteasome to measure if this degradation was unique to NOX5 or not.

Results

We found that NOX5 is degraded at around 4-6 hours and after the superoxide burst of ionomycin calcium salt, NOX5 was… We also found that the substrate that is a target of proteasomal degradation, P53 behaved…

Conclusion

As a result of this time-course experiment, we found **results**. It is very important to understand the various mechanisms that factor into the degradation of NOX5 as it is a crucial molecule for cell

signaling and overall physiological function. It is possible that over time, NOX5 turns on an autophagy mechanism that degrades itself without any interaction with the proteasome. It would be interesting to measure at what time point autophagy begins, in order to turn that mechanism off.

Sarah Rubenstein – University of Wisconsin Madison
Peter LaViolette, PhD
MCW Department of Radiology, Pathology

The Relationship Between Vasculature Characteristics and Prostate Carcinoma Progression

Background
Prostate cancer is a significant health concern affecting approximately one in eight men in their lifetime. The Gleason grade of a tumor indicates aggressiveness, with a lower grade signifying a less aggressive tumor. Histological characteristics of prostate vasculature may provide information about the presence and extent of tumors, making it a potential diagnostic tool. A previous study found that vessels encased in carcinoma had thicker and more cellular media compared to those in healthy tissue. We re-examined this hypothesis using modern image processing techniques.

Method
This study utilized high-resolution digital images of histological samples collected from twenty-seven patients, prepared with a hematoxylin and eosin (H&E) stain, and annotated by pathologists at MCW. The number of slides per patient varied between 3 and 15, with an average of approximately 8 slides. Image annotations isolated tumors (indicating Gleason grade) and vessels. High-resolution image tiles were taken from directly around the annotated regions of interest. A MATLAB-based, fully autonomous algorithm was developed to calculate the average media thickness, media-to-lumen ratio, and nuclei count of the vessel in each tile. We calculated media thickness by isolating the vessel's lumen, measuring the edge-to-lumen pixel distance, and averaging the measurements after correcting for oblique vessels. Nuclei count was obtained by masking out nuclei based on color, cleaning up noise, and counting the masked regions. To find the media-to-lumen ratio we divided the number of pixels in the media by those in the lumen. Linear mixed models were run on relevant relationships in SPSS statistics, using nested random effects of subject and slide to account for repeated measures.

Results
Of the 581 annotated vessels, 45 were excluded from analysis due to algorithm errors. Results showed that vessels further from tumors had generally thicker media (P=0.017) and more nuclei (P<0.001). Furthermore, among vessels within 1000 micrometers of a tumor, those closest to Gleason Grade 5 tumors had media thinner and less cellular than vessels closer to tumors of other Gleason grades. The media-to-lumen ratio was also larger in vessels encased by tumor (P=0.039).

Conclusion
Our results challenge the notion that vessels encased in carcinoma possess thicker and more cellular media. Instead, our data suggests that thinner and less cellular vasculature may serve as an indicator of advanced prostate cancer. A higher media-to-lumen ratio in vessels may also be indicative of nearby carcinoma. Future research is needed to resolve the conflicting outcomes between our study and a previous study that arrived at the opposite conclusion.

Max Lefebvre – University of Wisconsin-Stout
Jason W. Sidabras, Doc. rer. nat.
MCW Department of Biophysics

Technology Development for High-Resolution Pre-clinical Sodium Magnetic Resonance Imaging

Background

Sodium plays a crucial role in the body and is one of the essential electrolytes required for various physiological processes. Traditionally, Magnetic Resonance Imaging (MRI) primarily focuses on viewing the hydrogen (^{1}H) nuclei. Sodium (^{23}Na) MRI will provide additional information about sodium concentrations and contributions throughout the brain and body offering unique insights into several pathological and physiological processes that traditional MRI cannot accomplish. Applications include imaging various cancers, brain disorders, muscle physiology and disorders, cartilage degeneration, and fluid homeostasis. However, existing sodium MRI technologies face limitations in spatial resolution, preventing the ability to view fine details at the cellular level. The best spatial resolution to our knowledge is 1.4 x 1.6 x 1.7mm^3 with a scan time of 10 min.[3] There is therefore a critical need for developing high-resolution sodium pre-clinical MRI technologies to further advance our understanding of the brain and body. We will accomplish this by creating a coil based on the previous 1-loop surface coil paired with a 3-turn self-resonant spiral (SRS) design which has been shown to increase ^{1}H MRI resolution. [1] We believe that by using these design techniques we can acquire images with 4x resolution improvements.

Method

Two different types of Radio Frequency (RF) coils were designed. The first coil was a Helmholtz volume coil that was previously used for hydrogen at 3 T, which resonates at 128 MHz. We modified this coil to resonate at sodium's Larmour frequency of 105.9 MHz at 9.4T by changing the capacitance, inductance, and simplifying the coupling circuitry. The second coil designed was a novel 3-loop surface coil paired with a 17-turn SRS. We simulated these designs first using Ansys HFSS (High-Frequency Structure Simulator) and used that data to make the best design decisions.

Results

We simulated both designs and successfully lowered the frequency to 105.9MHz. The modified volume coil was tested in the 9.4T MRI scanner using a 250mM ^{23}Na sample. We got a clear signal by applying a substantial amount of power that would be potentially harmful to an animal. Mainly due to the coil being well under-coupled 105.9 MHz. The surface coil and SRS pair have been successfully built and bench tested.

Conclusion

From the volume coil, we learned more about the weaknesses of the design and are currently working on designing a new linear volume coil that will have better SNR and will be used with the surface coil design to further enhance the image quality. This ongoing project continues to advance both these coil designs to obtain sub-millimeter resolution. Overall, this project has contributed greatly to the goal of advancing sodium MRI.

Keywords: Sodium (^{23}Na) Magnetic Resonance Imaging (MRI), X-nuclei imaging, Surface Coil, Self-resonant Spiral, 9.4 T

References:

1. Mett, R. R., Sidabras, J. W., & Hyde, J. S. (2016). MRI surface-coil pair with strong inductive coupling.
2. Gast, L. V., Platt, T., Nagel, A. M., & Gerhalter, T. (2023). Recent technical developments and clinical research applications of sodium (23na) MRI.
3. Bajwa, A. A., Neubauer, A., Schwerter, M., & Schilling, L. (2022). 23na chemical shift imaging in the living rat brain using a chemical shift agent, tm[dotp]

Zhilan Wang – University of Illinois at Urbana - Champaign
Yang Wang, PhD
MCW Department of Radiology

Denoising Time Series ASL Data Using Machine Learning Approaches and Precise Estimation of CMRO2

Background

This study, driven by the need for enhancing data quality in Arterial Spin Labeling (ASL) analyses and precise estimation of the Cerebral Metabolic Rate of Oxygen Consumption (CMRO2) using ASL and BOLD timeseries data from MRI scans, examined the utility of machine learning algorithms. We utilize Extreme Randomized Tree and Multi-Layer Perceptron Network algorithms for CMRO2 estimation. For denoising process, we hypothesized that advanced denoising algorithms and computational methods could significantly reduce noise in ASL data. To test this, we employed 3D Convolutional Neural Networks (CNN) and Long Short-Term Memory (LSTM) Networks for denoising, implemented in Python.

Method

We applied state-of-the-art 3D Convolutional Neural Networks (CNN) and Long Short-Term Memory (LSTM) Network for denoising, aiming to optimize the temporal signal-to-noise ratio in ASL data. Concurrently, advanced computational methods, specifically the Extreme Randomized Tree and Multi- Layer Perceptron Network, were leveraged to refine CMRO2 estimation. These procedures were primarily executed in Python.

Results

The use of the machine learning approach led to a substantial improvement in the quality of ASL time series data. The introduced algorithms significantly reduced noise, providing cleaner and more accurate results. Furthermore, the adopted computational methods successfully provided precise estimations of CMRO2, aiding in the deeper understanding of brain metabolism and functionality.

Conclusion

This study showcases the successful amalgamation of machine learning techniques with traditional ASL and BOLD studies to considerably augment data quality. Additionally, our findings indicate that precise CMRO2 estimation can be achieved through advanced computational approaches, enriching our knowledge of brain functionality and metabolism. These encouraging results imply a promising scope for wider applications of these methodologies in future neurological research.

Keywords:

Machine Learning, Deep Learning, Arterial Spin Labeling (ASL), Time Series Denoising, 3D Convolutional Neural Networks (CNN), Long Short-Term Memory (LSTM) Networks, Cerebral Metabolic Rate of Oxygen Consumption (CMRO2), Extreme Randomized Tree, Multi-Layer Perceptron Network, Signal-to-Noise Ratio, Python

Lauren Schraufnagel – Miami University, Oxford
Gennadiy Gurariy, PhD; Ethan Duwell, PhD; Adam S. Greenberg, PhD
MCW Department of Biomedical Engineering

Optimization of Reverse Correlation: A Glimpse into Cognitive Processes

Background

Cognitive processes (e.g., memory, attention, etc.) are difficult to measure using purely behavioral methods. However, psychophysical reverse correlation (PRC) is a behavioral technique that can be used to uncover an internal template guiding visual behavior during cognitive tasks.[1] During PRC trials, participants are asked to make a perceptual judgement on a base image embedded under random noise. Noise fields are then mathematically combined to reveal the pixels that are most diagnostic of their perceptual decision. The resulting classification image (CI) represents the internal template utilized by participants to perform the task.

PRC typically requires approximately 10,000 trials per subject to produce significant results and is, thus, underutilized. We aimed to optimize PRC with the goal of reducing the number of trials needed. There exist numerous avenues of PRC optimization. Here, we optimize CI generation by exploring the mathematical algorithms used to combine noise fields. Specifically, we varied weighting schemes using reaction time (RT) under the assumption that it is a proxy for participant confidence.

Methods

One subject performed 9000 trials of a two-alterative forced choice task indicating the orientation of a Gabor grating. Gratings were tilted 10 degrees left or right with superimposed white noise . Task difficulty was held constant using a psychophysical staircase procedure . After data collection, classification images were generated using the following equation: CI = (NBase1,Resp2+ NBase2,Resp2)-(NBase1,Resp1+ NBase2,Resp1). This equation combines all noise resulting in one decision (right) and then subtracts all noise resulting in the opposing decision (left).

We separately analyzed correct and incorrect trials, because the mean RTs of each group differed by ~100ms, and applied 4 different weighting schemes. Our first method only used RTs within two standard deviations of the mean. Our second method used all data and applied separate weights to RTs above and below the mean. Our third method divided (& separately weighted) RTs into four increments, spanning two standard deviations above and below mean RT. Our fourth method divided/weighted RTs into four quartiles, excluding outliers. To compare efficacy, we computed the number of significant CI pixels via bootstrapping.

Results

CIs generated after separating correct and incorrect trials identified more diagnostic pixels and removed more background CI noise.

We also found that a linear weighting scheme (0.4/0.3/0.2/0.1) produced the most significant pixels with the quartile method and a 0.90/0.10 weighting scheme produced the most significant pixels with the weighted-average method. Thus, fastest RTs play the largest role in producing significant pixels, which may result from higher confidence on these trials.

Overall, the quartile method produced the most significant pixels.

Conclusion

We found that using the quartile method with a linear weighting scheme to generate CIs can potentially reduce the number of trials needed, thus making PRC more practical for visual cognition experiments.

References

1. L. Brinkman, A. Todorov & R. Dotsch (2017) Visualising mental representations: A primer on noise-based reverse correlation in social psychology, European Review of Social Psychology, 28:1, 333-361, DOI: 10.1080/10463283.2017.1381469

Jalyssa Gonzales - University of Colorado Boulder

Lezi E, PhD.

MCW Department of Cell Biology, Neurobiology, and Anatomy

Investigating the Role of Alzheimer's Disease Risk Genes in the Aging Process

Alzheimer's disease (AD) is an age-related neurodegenerative disease characterized by the progressive decline of cognitive function. While the etiology of AD pathogenesis remains elusive, in recent years, genome-wide association studies have identified a fair number of genes associated with AD risk. However, there is still a critical knowledge gap regarding the contribution of these genetic factors to AD pathogenesis. This project aims to investigate the role of these risk genes in aging, an important factor in AD onset. To study this, we used *Caenorhabditis elegans* (*C. elegans*) as a model, which possess orthologs for more than half of the identified risk genes. Lifespan assays were conducted to determine the median lifespan of *C. elegans* when specific genes were knocked down using RNA interference. The genes selected for this study include *acn-1*, *amph-1*, and *tsp-12*, which are known orthologs of AD risk genes *ACE*, *BIN1*, and *TSPAN14*, respectively. Notably, *ACE* and *BIN1* have been linked to late-onset Alzheimer's disease, the most prevalent Alzheimer's subtype. To knockdown the expression of these genes, we utilized RNA interference which we established by feeding the *C. elegans Escherichia coli* expressing double-stranded RNA. Daily monitoring of the animals assessing their survival was then performed to determine the median lifespan of each group in comparison to an empty vector control group. Among the genes that we tested, *C. elegans* with reduced *acn-1* expression exhibited a significantly altered lifespan, with a median lifespan of 17 days compared to 21 days in the control group ($p=0.0001$). On the other hand, the group with reduced *amph-1* expression had a median lifespan of 21 days ($p=0.0731$), and the group with reduced *tsp-12* expression had a median lifespan of 21 days ($p=0.0958$), similar to that of control animals. The data obtained throughout this study suggests that *acn-1/ACE* may play a

significant role in organismal aging process. This finding underscores the potential importance of this gene in the context of AD onset risk. Further studies can be conducted to investigate whether the shortened lifespan and aging effects of this gene are accompanied by neurodegeneration to achieve a more complete understanding of *acn-1/ACE* as it relates to Alzheimer's disease.

Keywords:

Alzheimer's disease, *C. elegans*, aging.

Abby Bendixen – Connecticut College
Pui-Ying (Penny) Lam, PhD
MCW Department of Cell Biology, Neurobiology and Anatomy; Neuroscience Research Center

---

Characterization of Calcium Transients in Macrophage chemotaxis using *Danionella cerebrum*

Background

Macrophages play an important role in the innate immune response, performing a diverse set of functions. In response to signals released at a site of injury, macrophages migrate to the wound in a process called chemotaxis. The intracellular signaling of chemotaxis is not clearly understood. Ca^{2+}, one of the most prominent cellular signaling molecules, can have great effects on cellular responses and functions, including motility. Several receptors and channels regulate Ca^{2+} levels both intra- and extra-cellularly. Among these are the purinergic P2 receptors, IP_3 receptors, CRAC channels (associated with the STIM1 protein), and TRPC channels. *D. cerebrum* was utilized as an animal model due to its lifelong optical transparency, allowing for the visualization of cellular events *in vivo*. Preliminary data showed that dynamic Ca^{2+} transients in macrophages occurred during wound response. To test the role of Ca^{2+} signaling in macrophage chemotaxis in response to injury, and to identify the source of these Ca^{2+} transients, inhibitors targeting specific Ca^{2+} channels were used in a tail fin injury assay. The total number of macrophages migrating to and at the wound site were quantified to determine involvement of these Ca^{2+} channels in macrophage wound response.

Method

To observe the role of several selected Ca2+ channels in macrophage movement, the Tg(mpeg1:dendra2) line of D. cerebrum was utilized. The mpeg1 promoter drives expression of the fluorescent protein dendra2 exclusively in macrophages and microglia, allowing for cell visualization. Three day post fertilization (dpf) larvae were pre-incubated in a solution of E3 and an inhibitor for one hour, injured via tail transection, incubated in the same inhibitor solution for two hours, then fixed for two hours before imaging. The compounds included KN-62 (P2X7 antagonist), 2-APB (IP3R antagonist, TRP channel modulator), A740003 (P2X7 antagonist), SKF-96365 (STIM1 inhibitor), PPADS (P2Y antagonist), and apyrase (hydrolyzes extracellular ATP). Spinning disk confocal microscopy was utilized to image the samples, creating a 3-D image that was analyzed using Imaris image analysis software. The number of cells present were counted and grouped: cells within 20μm and cells between 21μm to 350μm from the wound site.

Results

The results from five independent experiments were compiled and graphed based on percent of cells at the wound site compared to percent of cells in migration. There was a significant difference between percentage of cells in migration in the apyrase group compared to the control group (DMSO).

Conclusion

The difference in migration levels of macrophages between the control and apyrase groups indicates involvement of extracellular ATP in macrophage chemotaxis, suggesting a potential role of purinergic receptors in macrophage migration.

Eliam Sanchez – University of Colorado Boulder
PI: Dr. Michael Widlansky, MD, MPH, FAHA, FACC
Post-Doctoral Fellow: Dr. Michael Aljadah, MD
MCW Department of Medicine, Division of Cardiovascular Medicine

---

Impact of Lactobacillus plantarum 299v probiotic supplementation on vascular function and exercise capacity in chronic heart failure with reduced and preserved ejection fraction.

Background

Heart Failure (HF) is a clinical syndrome characterized by orthopnea, dyspnea at rest or on exertion, lower extremity and abdominal swelling, and vascular congestion.[1] HF is one of the leading causes of inpatient admissions and has high mortality. The pathophysiology of HF revolves around impairment in left ventricular relaxation, impaired ejection fraction (EF) of blood, or both. Persistent inflammation is an important pathogenic factor of chronic heart failure and results in production and release of pro-inflammatory cytokines, activation of the complement system, and autoantibodies, all which participate in the destruction and dysfunction of the endothelial vascular layer.[2] Endothelial dysfunction is well-documented in patients with reduced (EF<40%) and preserved (EF>50 %) ejection fraction, due to the reduction of bioavailable NO seen in persistent inflammatory states[2]. In fact, the severity of endothelial dysfunction is a predictor of mortality and adverse outcomes, and this can be quantified using cardiopulmonary exercise testing (CPET), flow-mediated dilation (FMD), pulse-wave velocity (PWV), and measurement of inflammatory biomarkers.[3 4 5]. However, despite a known inflammatory component to HF, clinical trials with anti-inflammatory therapies have thus far been disappointing. Previous studies by Dr. Widlansky have showed that modulating the gut microbiome, a known potentiator of inflammation Lp299v probiotic decreased systemic inflammation in men with stable coronary artery disease and also improved vascular endothelial function by the measurement techniques described above.[3 6 7] We therefore set out to measure whether modulation of the gut microbiome with Lp299v, a known beneficial bacterial strain, could reduce inflammation and improve exercise capacity in patients with HF.

Methods:

This is a randomized, double-blinded, parallel-arm pilot study containing 20 individuals with HF, 10 of whom have reduced ejection fraction (HFrEF) and 10 who have preserved ejection fraction (HFpEF).

After selection via preset inclusion criteria and screening based on extensive exclusion criteria, subjects are randomized to Lp299v capsules or potato starch capsules for 12 weeks. The subjects then complete two subsequent study visits 12 weeks apart for pre-and post-testing that include echocardiograms, CPET, FMD, PWV, blood tests, and stool tests.

Results / Conclusion

Thus far, 10 screening visits have occurred yielding 3 enrolled patients in the HFrEF arm. More screening visits are scheduled for both the HFrEF and HFpEF arms to see if patients qualify. The study is still ongoing, and methods to recruit patients include institutional review board (IRB) approved use of the electronic medical record, internet advertisements, flyer advertisements placed in the clinics, and approaching patients directly after clinic visits. When the pilot study concludes, we anticipate reduction of systemic inflammation, improvements in vessel function, reduction in

vascular stiffness, and improvement in exercise capacity in patients with HF randomized to the Lp299v group. This data will later be used for a higher powered, NIH funded study.

References:

1. Kubrychtova V, Olson TP, Bailey KR, Thapa P, Allison TG, Johnson BD. Heart rate recovery and prognosis in heart failure patients. *Eur J Appl Physiol*. 2009;105(1):37-45. doi:10.1007/s00421-008-0870-z

2. Dick SA, Epelman S. Chronic Heart Failure, and Inflammation: What Do We Really Know? Circ Res. 2016 Jun 24;119(1):159-76. doi: 10.1161/CIRCRESAHA.116.308030. PMID: 27340274.

3. Widlansky, M. E., Gokce, N., Keaney, J. F., & Vita, J. A. (2003, October). The clinical implications of endothelial dysfunction:42(7) 1149-1160 https://www.jacc.org/doi/abs/10.1016/s0735-1097%2803%2900994-x

4. Arena R, Guazzi M, Cahalin LP, et al. Revisiting cardiopulmonary exercise testing applications in heart failure: aligning evidence with clinical practice. Exerc Sport Sci Rev. 2014 Oct;42(4):153-60. doi: 10.1249/JES.0000000000000022. PMID: 25061999.

5. Heitzer T, Baldus S, von Kodolitsch Y, et al. Systemic endothelial dysfunction as an early predictor of adverse outcome in heart failure. Arterioscler Thromb Vasc Biol. 2005 Jun;25(6):1174-9. doi: 10.1161/01.ATV.0000166516.52477.81. Epub 2005 Apr 14. PMID: 15831810.

6. Hofeld BC, Puppala VK, Tyagi S, et al. Lactobacillus plantarum 299v probiotic supplementation in men with stable coronary artery disease suppresses systemic inflammation. Sci Rep. 2021 Feb 17;11(1):3972. doi: 10.1038/s41598-021-83252-7. PMID: 33597583; PMCID: PMC7889883.

7. Malik M, Suboc TM, Tyagi S, et al. Lactobacillus plantarum 299v Supplementation Improves Vascular Endothelial Function and Reduces Inflammatory Biomarkers in Men With Stable Coronary Artery Disease. Circ Res. 2018 Oct 12;123(9):1091-1102. doi: 10.1161/CIRCRESAHA.118.313565. PMID: 30355158; PMCID: PMC6205737.

Nathaniel Troemel – University of Georgia
Michael Widlansky,
MCW Department of Cardiology

Effect of Probiotics (Lp299v) on Vascular Age & Endothelial Function in Healthy Older Adults

Background

Cardiovascular disease causes significant morbidity and mortality in an ever-growing aging population. Three major mechanisms have been identified that detect advancement of vascular aging, which can lead to CVD. These include impaired endothelium-dependent vasodilation, increased vascular stiffness, and maladaptive arterial wall remodeling that leads to increased plaque vulnerability. Recent studies have improved our understanding of the crucial role gut microbiome plays in regulating vascular health. A study conducted by our team demonstrated that once daily supplementation of the probiotic *Lactobacillus plantarum 299v* (Lp229v) had favorable effects on the vascular health of those with coronary artery disease (CAD). These effects include improvement of endothelium-dependent vasodilation and reduced systemic inflammation and inflammatory signaling. While promising, we cannot generalize these findings to the general population due to complex pathophysiology and medication interactions. This study aims to measure the effect of Lp299v supplementation on endothelial function, vascular stiffness, and maladaptive remodeling in healthy men and women to further ascertain the vascular benefit of this probiotic. It also aims to determine the feasibility of Lp299v intervention in healthy older adults, as well as quantify its impact on systemic and endothelial inflammation.

Methods

For this pilot study, 10 males and 10 females without pre-existing risk factors for CAD were recruited. Due to vascular function improvements made during exercise, participants taking over 7500 steps/day were excluded. Participants are screened using vitals and labs. If eligible, baseline measurements for vascular health, including flow-mediated dilation (FMD), pulse wave velocity (PWV), inflammatory markers, and stool sample are collected. Participants are randomized into placebo or probiotic group. They supplement for 12 weeks and return for visit 3, where vascular function is again measured.

Results

Due to the early stage of this study, there are no results yet. However, we anticipate improvement in vascular endothelial function, reduced vascular stiffness, and increased resting laminar shear stress in the brachial artery. We also anticipate reduced pro-inflammatory cytokine and endothelial biomarkers. These expectations are scientifically based on our understanding of the mechanism of Lp299v and its effect on vascular function in those with CAD.

Conclusion

Overall, our hypothesis poses that the link between the gut microbiome and vascular health may be the gateway to pharmacological, non-invasive treatments and preventions of vascular diseases. Through supplementation of Lp229v, we pose that there will be marked improvements in vascular health and function seen via improved endothelium-dependent vasodilation, along with reduced systemic inflammation, arterial stiffness, and maladaptive vascular remodeling.

John Motter - Bowling Green State University

Dr. Dara Frank

MCW Department of Microbiology and Immunology

Characterization of the Structure and Function of *Pseudomonas aeruginosa* Toxin, ExoU

Background

ExoU is an A2 phospholipase produced by the human pathogen *Pseudomonas aeruginosa*. Expression of ExoU during infection is associated with more severe illness, especially in vulnerable patient populations such as individuals on ventilator assistance. Previous work in the field has produced a crystal structure of ExoU bound to its chaperone, SpcU, however, the enzyme is considered inactive in this state. Production of a model of active ExoU has proven difficult, namely due to the flexibility of the protein and its size limiting *in vitro* efforts. Structural analysis of the active form of ExoU could enable drug design. We hypothesize that if an enzymatically active complex of ExoU and its coenzyme ubiquitin can be generated, the complex will be stable enough to undergo imaging attempts through crystallography or cryoEM.

Methods

To produce protein for analysis, we transformed *E.coli* with plasmids containing expression constructs of our protein of interest. A combination of lysis, centrifugation, and chromatography was used to purify protein products. Enzyme assays quantified enzymatic activity by measuring the fluorescence of PED6, the fluorescent product from cleavage of a quencher molecule from a modified enzyme substrate. Product purity and concentration were measured using A280 absorbance and SDS-polyacrylamide gel electrophoresis with Coomassie staining or Western blot analysis. Computational structural models were generated with AlphaFold *de novo* folding, and molecular dynamics simulations were generated using GROMACS.

Results

ExoU and ubiquitin mutant complex R515C-A46C forms a stable complex, however, these complexes are enzymatically inactive except in the presence of unbound ubiquitin. N-terminal deletions of ExoU have a lower activity than wild-type ExoU, butExoU but show no significant difference in activity between mutants or between complexed mutants . Attempts to form an ExoU-ubiquitin complex with non-covalently linked ubiquitin have been unsuccessful.

Conclusion

Enzyme-coenzyme complexes were formed between ExoU R515C mutants and ubiquitin mutant A46C that are connected by a disulfide bond between cysteine residues placed at the ExoU-ubiquitin binding interface. Although this complex occupies the predicted ubiquitin binding interface, which is indicated by disulfide bond formation, it is enzymatically inactive. This complex can be activated using free ubiquitin, however, the mechanism behind this is unknown. Since enzymatically active ExoU exists in the absence of its chaperone SpcU in vivo, deletions of the predicted SpcU binding interface at the amino terminus were generated in attempts to increase ExoU stability. R515C mutants with N-terminal deletions have an elevated melting point, which suggests that they are more stable . Further research is needed to develop an enzymatically active complex, as well as to understand the mechanism by which ubiquitin activates ExoU in covalent complexes.

Ollie Kamalei – Brown University
Bonnie Dittel, PhD
MCW Department of Microbiology and Immunology

Developing a Retroviral Vector for TL1A Expression in IgD Low B Cells

Multiple Sclerosis (MS) is an increasingly prevalent autoimmune disorder of the central nervous system (CNS) characterized by demyelination of brain and spinal cord nerves (*Multiple Sclerosis (MS)*, n.d.). $FoxP3^{+}CD4^{+}$ regulatory T cells (Tregs) play a pivotal role in regulating autoimmunity by quieting inflammatory responses (Vignali et al., 2008). Our lab previously identified a novel subset of IgD low regulatory B cells (BD_L) that stimulate Treg proliferation in a GITRL-dependent manner, thereby negatively regulating the severity of autoimmunity in the mouse model of MS, experimental autoimmune encephalomyelitis (EAE) (Ray et al., 2019). Our lab has shown BD_L overexpressing GITRL increased Treg count 4-fold compared to WT BD_L. Another TNF superfamily receptor that induces Treg expansion upon stimulation is TNFR25, which is highly expressed on Tregs and has been shown to increase *in vivo* Treg expansion two-fold (Wolf et al., 2016). BD_L however are not known to express TL1A, the ligand for TNFR25 (Richard et al., 2015). We hypothesize BD_L overexpressing TL1A will increase Treg proliferation compared to wild-type BD_L, similar to BD_L overexpressing GITRL. To test this, we developed a retrovirus cloning vector for the purpose of increasing surface TL1A expression in BD_L. Mouse stem cell virus puromycin-resistant (MSCV Puro) retrovirus vector and TL1A gene fragment were cut with restriction enzymes and ligated together before transduction into chemically competent *E. coli* cells. Plasmid DNA was harvested and recut with restriction enzymes before visualization on agar gel, which suggested the TL1A gene was successfully inserted into the vector. However, the results of additional verification by Sanger sequencing were inconclusive. A different approach, known as TA cloning, will be employed to ensure stable insertion of the TL1A gene into the vector. Future work aims to transfect mouse hematopoietic stem cells with our recombinant retrovirus. Transfected stem cells will be transplanted into mice, which after verification will be adoptively transferred to B cell-deficient mice (B10.PLuMT). We expect to observe increased Treg expansion in uMT mice that receive our BD_L overexpressing surface TL1A (BD_L-TL1A) compared to WT BD_L. This work will serve as a proof-of-concept in the development of a transgenic BD_L-TL1A mouse and will aid in pursuing the worth of overexpressing TL1A on a BD_L-based adoptive cell therapy for treatment of autoimmune disease.

Kondelkova, K., Vokurková, D., Krejsek, J., Borska, L., Fiala, Z., & Andrys, C. (2010). Regulatory T cells (Treg) and Their Roles in Immune System with Respect to Immunopathological Disorders. *Acta Medica*, *53*(2), 73–77. https://doi.org/10.14712/18059694.2016.63

Multiple Sclerosis (MS). (n.d.). Johns Hopkins Medicine. https://www.hopkinsmedicine.org/health/conditions-and-diseases/multiple-sclerosis-ms

Ray, A., Khalil, M. I., Pulakanti, K., Burns, R. T., Gurski, C. J., Basu, S., Wang, D., Rao, S., & Dittel, B. N. (2019). Mature IgDlow/- B cells maintain tolerance by promoting regulatory T cell homeostasis. *Nature Communications*, *10*(1). https://doi.org/10.1038/s41467-018-08122-9

Richard, A. F., Ferdinand, J. R., Meylan, F., Hayes, E., Gabay, O., & Siegel, R. M. (2015). The TNF-family cytokine TL1A: from lymphocyte costimulator to disease co-conspirator. *Journal of Leukocyte Biology*, *98*(3), 333–345. https://doi.org/10.1189/jlb.3ri0315-095r

Vignali, D. A., Collison, L. W., & Workman, C. J. (2008). How regulatory T cells work. *Nature Reviews Immunology*, *8*(7), 523–532. https://doi.org/10.1038/nri2343